Synthesis of Dense TiC-Ti Cermets via SHS and QIP

Student: JunKun Ma

Advisor: E.A. Olevsky (SDSU)

M.A. Meyers (UCSD)

Dissertation for partial satisfaction of the requirements for the degree of Doctor of Philosophy in Engineering Science / Applied Mechanics

07/02/2004

Acknowledgements

- National Science Foundation (NSF) Career Grant to Professor E.A. Olevsky.
- JDP program between SDSU and UCSD
- Advisor Professor E.A. Olevsky (SDSU)
- Advisor Professor M.A. Meyers (UCSD)
- Dr. A. Maximenko (SDSU)
- Committee members

  Prof. D. J. Benson (UCSD)

  Prof. K. B. Morsi (SDSU)

  Prof. M. L. Rudee (UCSD)

Outline

- Introduction.
- Theoretical modeling.
- Experiments.
- FEM simulations.
- Conclusions.
- Future work.

Introduction of SHS and QIP

Self-propagating High-temperature Synthesis (SHS)

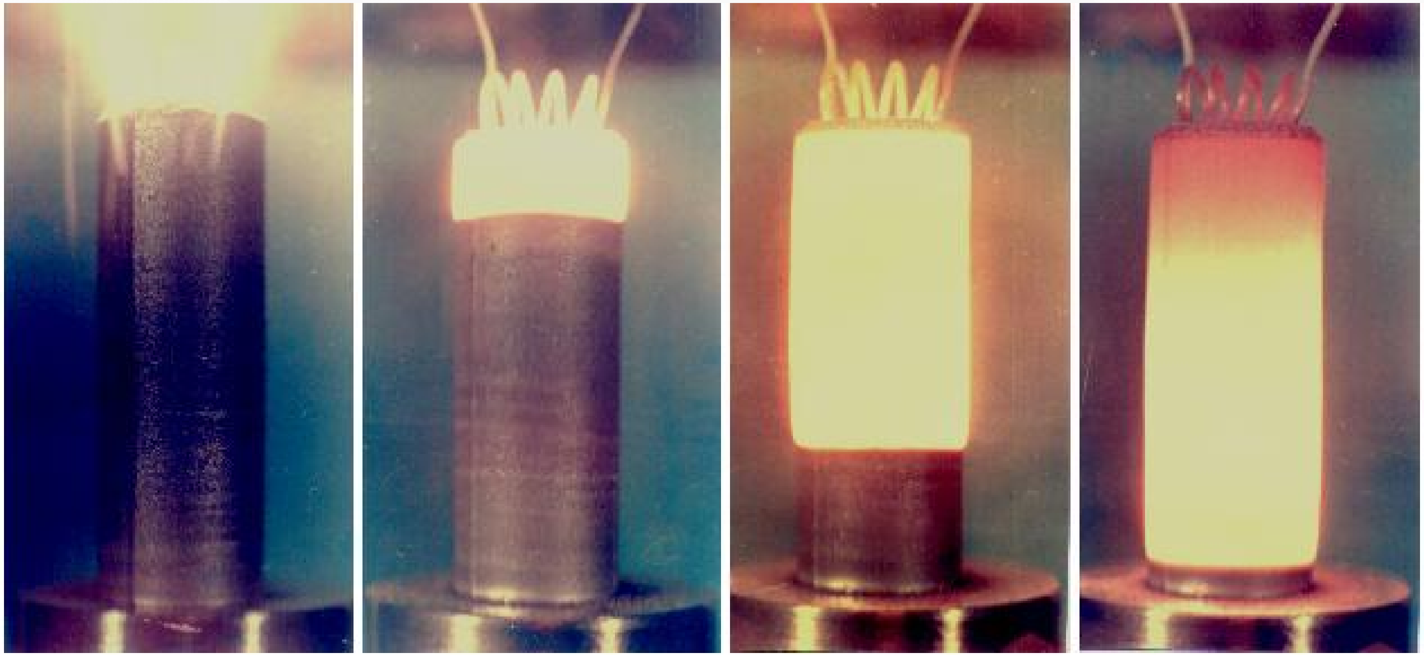

t=0s t=0.1s t=2.7s t=4.0s

The synthesis of materials/compounds is achieved in wave of chemical reaction/combustion that propagates over starting reactive mixture via layer-by-layer heat transfer

Photo courtesy: http://www.ism.ac.ru/handbook/shsf.htm

SHS Product and Applications

- Composites materials. ($TiC+Al_2O_3$)
- Materials with specific properties.(BaTiO3)
- Cutting tools and polishing powder. (TiC)
- Shape memory alloys. (TiNi)
- Intermetallic compounds. (Ni Aluminides)
- Thin films and coatings, (TiB_2)
- Heating elements. ($MoSi_2$)
- Bioengineering implants. (Ti+TiB)

Advantages of SHS

- **Volatilizing low boiling point impurities.**
- **Avoids expensive processing facilities.**
- **Short operating and processing time and cost.**
- **Inorganic materials can be synthesized and consolidated into final product in one step.**
- **Obtain specific phase of the materials.**

SHS Problems and Challenges

- **Final mechanical and physical properties (excessive porosity).**
- **Explosive character of SHS.**
- **Short processing time -- hard to control.**
- **High temperatures and rapid cooling cause operational difficulty.**

Solution: Post-Combustion Densification: QIP (Quasi-Isostatic Pressing).

Different Consolidation Setups

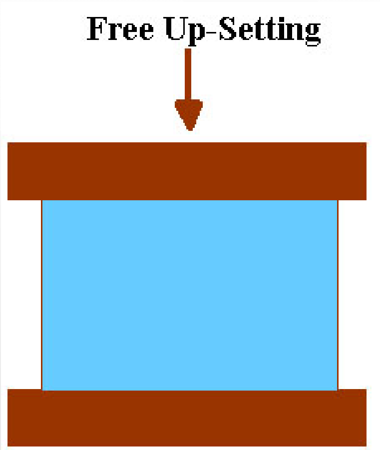

Distortion

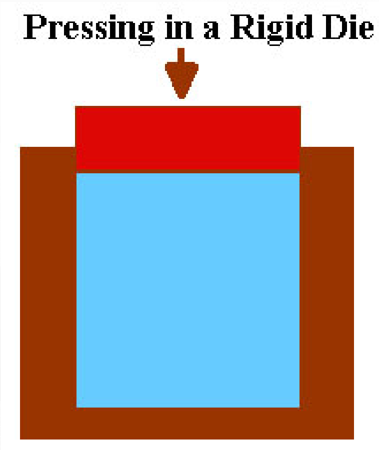

Cooling, Adhesion

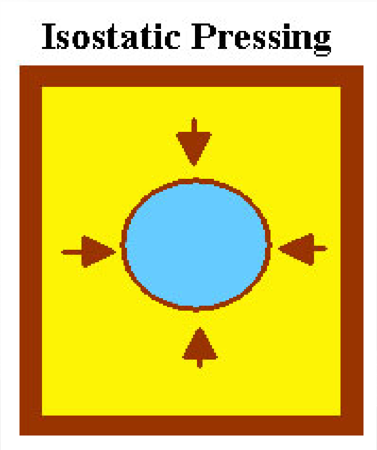

Expensive

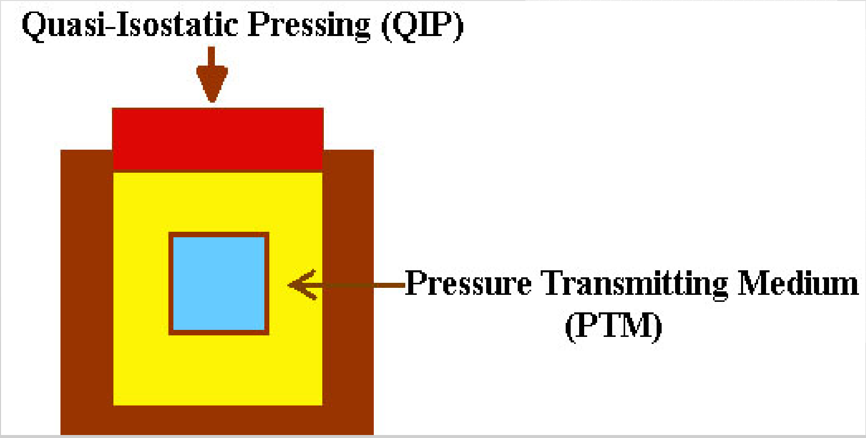

Cheap, Low cooling rate
Moderate shape change
(Compressive PTM)

Controlling Parameters of SHS

- **Reactants composition.**
- **Time between combustion and consolidation**
- **Consolidation load and schematics.**
- **Particle size and shape.**
- **Particle preparation and handling.**
- **Green density of sample.**
- **Combustion temperature and rate.**
- **Gravity.**

Generic Research Goal

Net-shape fabrication of dense TiC-Ti cermets

Research Route

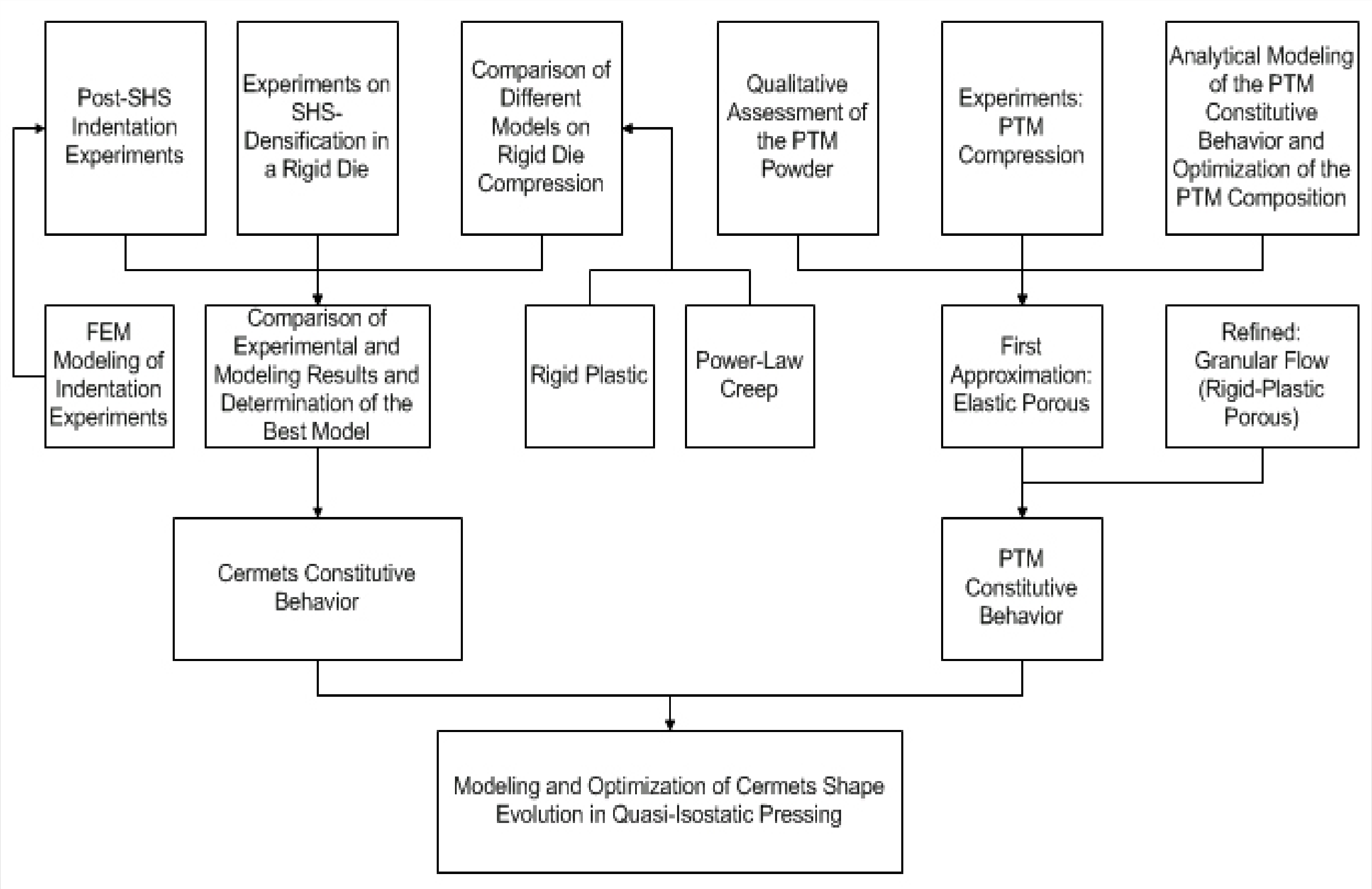

Research Components

- **Theoretical Modeling**

  Analysis of applicability of various models, finding first model approximations for process and material parameters.

- **Experiments**

  Determination of optimal process and material parameters:

  Optimal composition of the cermet, optimal composition of the PTM, time scheme of combustion and densification procedure.

- **FEM Simulation**

  Controlling and optimizing the shape change under QIP.

Scientific Novelties

- **For the first time, dense TiC-Ti cermets is synthesized by using SHS and QIP technique.**
- **As first approximation, an elastic model describing the constitutive behavior of PTM is created. The optimal composition of PTM was determined.**
- **Technical parameters that are critical in the fabrication of dense net-shape final products via SHS and QIP, such as cermet composition, time window between combustion and densification, densification load, particle size, have been investigated.**
- **A FEM code based on the nonlinear-viscous porous bodies theory developed by Dr. E.A. Olevsky and Dr. A. Maximenko has been further developed to simulate the QIP process.**
- **Both the constitutive behavior of the TiC-Ti and the PTM have been implemented into commercial FEM package ABAQUS to simulate and optimize the densification process of the TiC-Ti cermet in QIP setup.**

Theoretical Modeling

Objective and Tasks

- **Understand the constitutive behavior of porous cermets during high-temperature densification.**

1. **Determine the constitutive parameters: shear and bulk moduli for porous materials used in the study.**
2. **Model the porous cermets as a rigid-plastic material and compare the results with experimental results .**
3. **Model the porous cermets as a power-law creep material and compare the results with experimental results.**
4. **Determine which model of shear and bulk moduli has best agreement with experimental results and whether rigid-plastic models or power-law creep models for porous cermets should be employed**

Objective and Tasks (continue I)

- **Understand the constitutive behavior of PTM**

1. **Conduct compression experiments of PTMs with different concentrations of fused alumina and graphite.**
2. **Model the compressive constitutive behavior of PTM with respect to porosity of the PTM and composition of fused alumina and graphite in the PTM**

Objective and Tasks (continue II)

- **Model and optimize the densification process of the porous cermets in QIP setup.**

1. **Determine related materials parameters of the porous cermets needed in the modeling. Conduct after combustion indentation experiments.**
2. **Model the constitutive behavior of the porous cermets in QIP densification mode.**
3. **Determine the optimal PTM concentration in order to obtain net-shape final products with a high final density**

The Main Constitutive Relationship

Strain rate component

Bulk modulus:
Resistance to the volume change
<u>function of porosity</u>

Shear modulus:
Resistance to the shape change
<u>function of porosity</u>

$$\sigma_{ij} = \frac{\sigma(W)}{W}\left[\varphi \dot{e}_{ij} + \left(\psi - \frac{1}{3}\varphi\right)\dot{e}\delta_{ij}\right] + P_L \delta_{ij}$$

Volume strain rate

Generalized viscosity:
corresponds to the constitutive properties of particle material

Effective sintering stress:
<u>function of porosity</u>

externally applied stresses | material resistance | sintering

Linear Viscous: $\sigma(W) = 2\eta_0 W$

Rigid Plastic: $\sigma(W) = \sigma_y$

Power Law Creep: $\sigma(W) = AW^m$

$$W = \frac{1}{\sqrt{1-\theta}}\sqrt{\varphi\dot{\gamma} + \psi\dot{e}^2}$$

Yield Criterion of Porous Materials

$$\frac{P^2}{\psi}+\frac{\tau^2}{\varphi}=\delta\sigma_{y_0}^2$$

Where P is the first invariant of stress tensor, τ is the second invariant of stress tensor deviator. σ_{y0} is the yield stress of the fully dense material. For the case of uniaxial compression of an axisymmetric body, it is assumed that $d\varepsilon_r = d\varepsilon_\theta = 0$ and $\sigma_r=\sigma_\theta = [v/(1-v)]\sigma_Z$ (where v is Poisson's ratio) . The stress tensor invariant are then given by:

$$P=\frac{\sigma_r+\sigma_\theta+\sigma_Z}{3}=\frac{1}{3}\left(\frac{1+v}{1-v}\right)\sigma_Z$$

$$\tau=\sqrt{\frac{1}{3}\left[\left(\sigma_r-\sigma_\theta\right)^2+\left(\sigma_\theta-\sigma_z\right)^2+\left(\sigma_z-\sigma_r\right)^2\right]}=\sqrt{\frac{2}{3}}\left(\frac{1-2v}{1-v}\right)\sigma_z$$

Different Models for Constitutive Parameters of Porous Materials

Models	φ	ψ	δ
Skorohod	$\frac{1}{\rho^2}$	$\frac{3}{2}\frac{(1-\rho)}{\rho^3}$	ρ
Kuhn&Downey	$\frac{3}{2}\rho\left(2+\rho^2\right)$	$\frac{9}{2}\rho(3-\rho)(1-\rho)$	ρ
Gurson	$\frac{9}{2}\frac{1-(1-\rho)^2}{1+(1-\rho)^3}$	$\frac{9}{2}\frac{(1-\rho)^2\left(1-(1-\rho)^2\right)}{1+(1-\rho)^3}$	ρ
Doraivelu	$\frac{3\left(2+\rho^2\right)}{2\left(2\rho^2-1\right)}$	$\frac{9(3-\rho)(1-\rho)}{2\left(2\rho^2-1\right)}$	1
McMeeking & Sofronis	$\left(\frac{\rho}{2-\rho}\right)^{\frac{2}{m+1}}$	$\frac{2}{3}\left(\frac{1-(1-\rho)^m}{m(1-\rho)^m}\right)^{\frac{2}{m+1}}$	ρ

Where m and ρ are strain sensitive factor and relative density respectively

Stress-Density Relationship for Rigid-Plastic Models

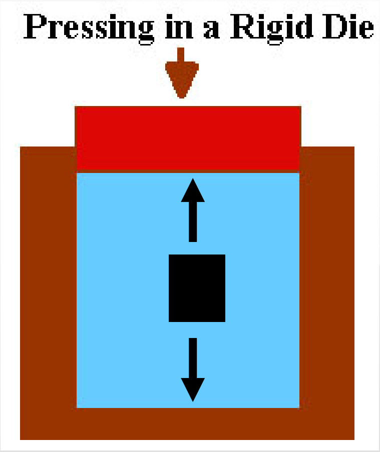

Doraivelu:

$$\sigma_Z(\rho,T) = -\sigma_{y_0}\left(1-\frac{T-T_0}{T_{am}-T_0}\right)\left(\frac{\rho^2-\rho_i^2}{1-\rho_i^2}\right)^{\frac{1}{2}}\left[\frac{\left(2-\rho^2\right)}{\left(1-\rho^2\right)\left(2+\rho^2\right)}\right]^{\frac{1}{2}}$$

Kuhn&Downey:

$$\sigma_Z = -\frac{\sqrt{2}}{3}\sigma_{y_0}\left(1-\frac{T-T_0}{T_{am}-T_0}\right)\left(\frac{2}{2+\rho^2}+\frac{1}{(1-\rho)(3-\rho)}\right)^{\frac{1}{2}}$$

Skorohod:

$$\sigma_Z = -\sqrt{\frac{2}{3}}\sigma_{y_0}\left(1-\frac{T-T_0}{T_{am}-T_0}\right)\left(\frac{\rho^{\frac{3}{2}}}{(1-\rho)^{\frac{1}{2}}}\right)$$

Gurson:

$$\sigma_Z = -\frac{\sqrt{2}}{3}\sigma_{y_0}\frac{1}{1-\rho}\left(1-\frac{T-T_0}{T_{am}-T_0}\right)\left[\left(\rho+(1-\rho)^2\right)\frac{2(1-\rho)^2+1}{3}\right]^{\frac{1}{2}}$$

Where T_0 = 25 ^{0}C is the room temperature, T_{am} = 2080 ^{0}C which is the liquid phase temperature for alumina. ρ is the relative density.

Comparison of the constitutive models for axial strain compression of hot porous materials and the corresponding experimental curve.

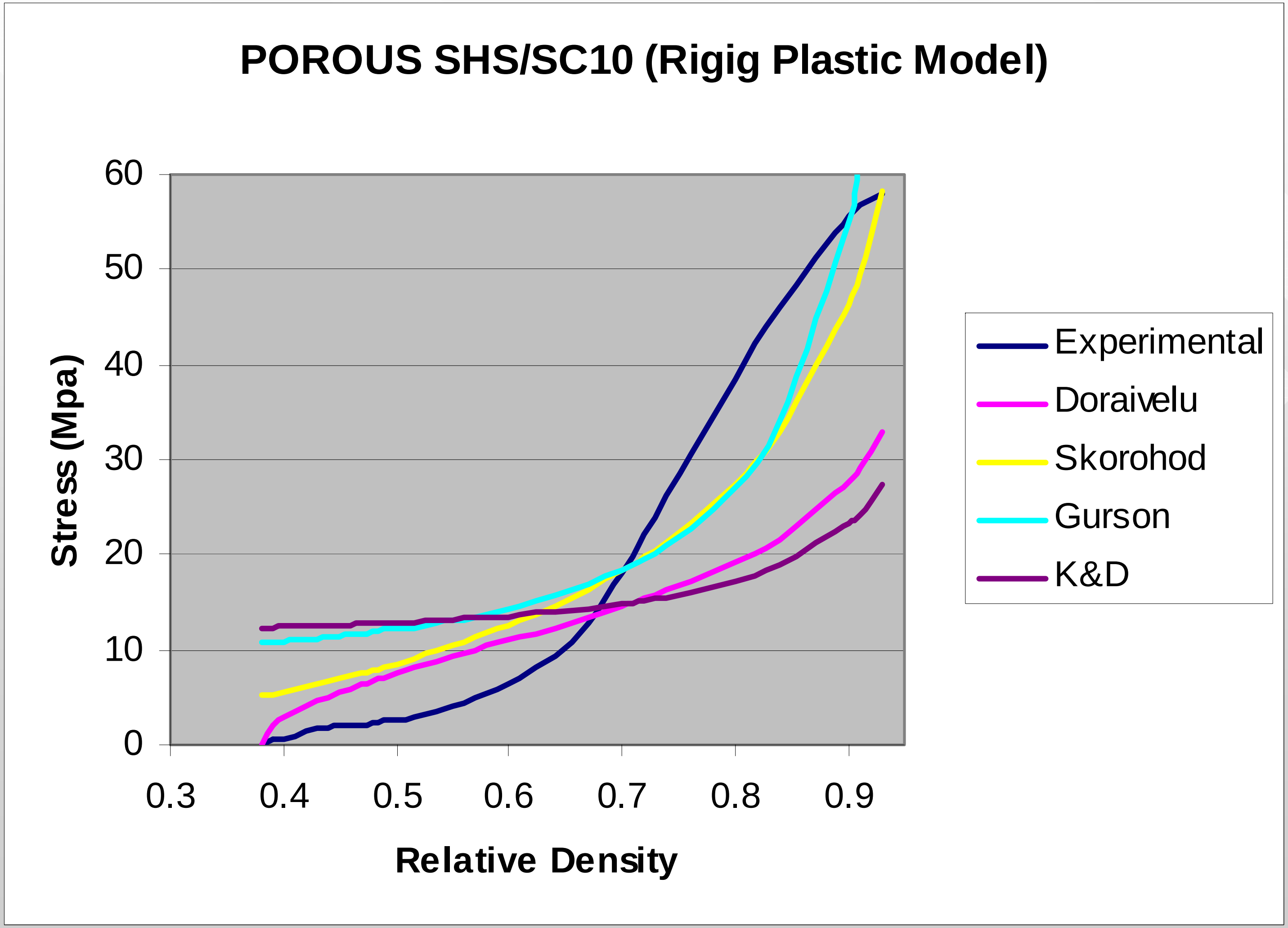

Comparison of the constitutive models for axial strain compression of hot porous materials and the corresponding experimental curve.

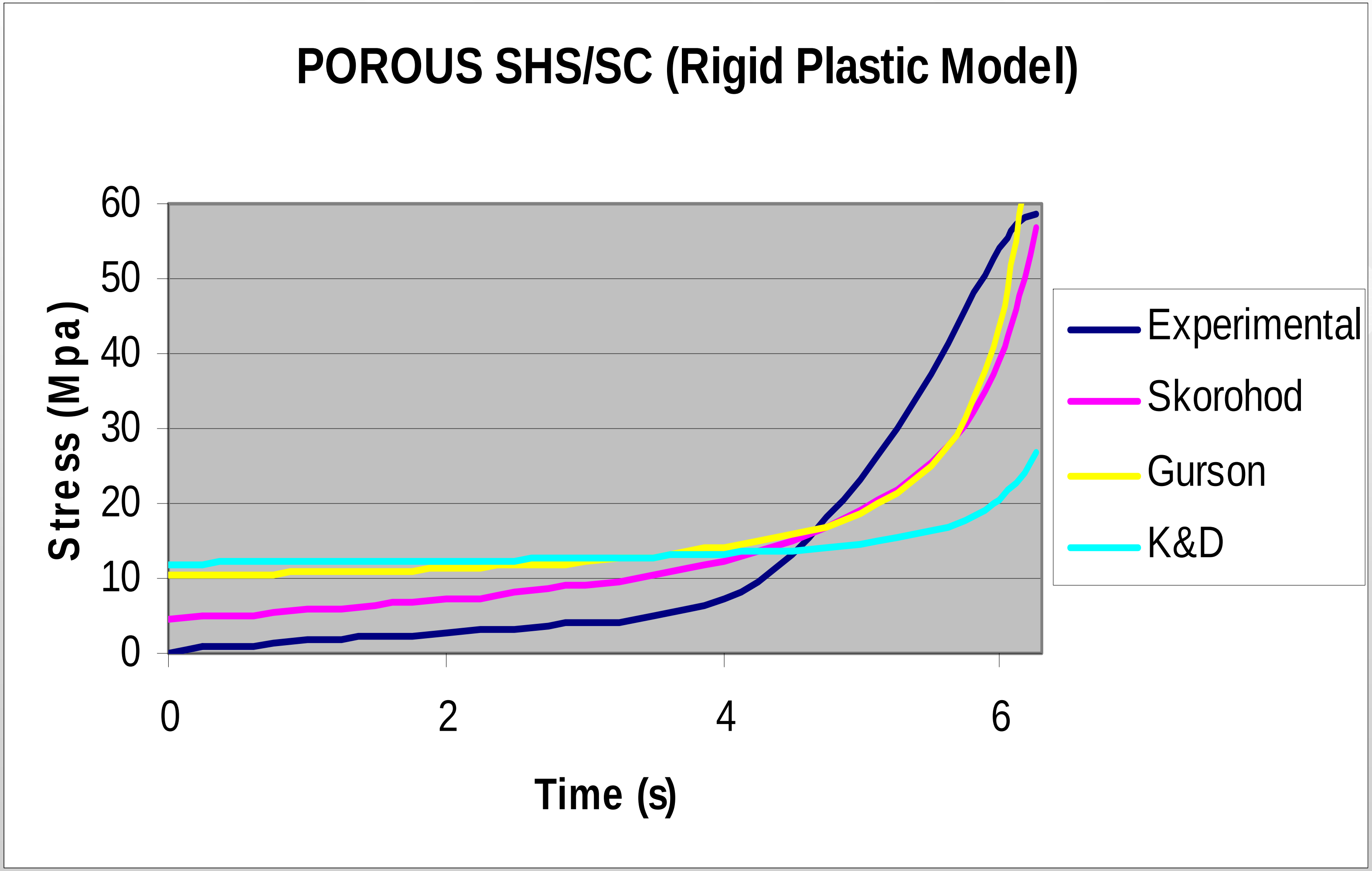

Indentation for Determination of *A* and *m*

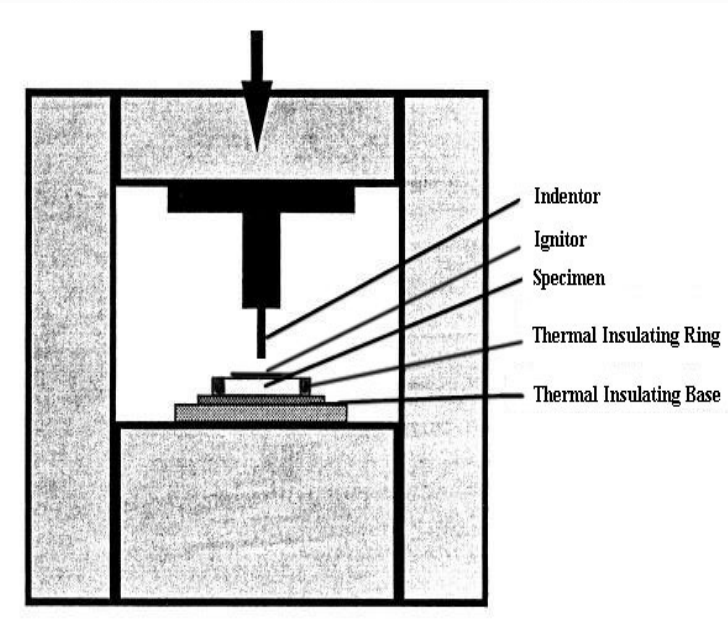

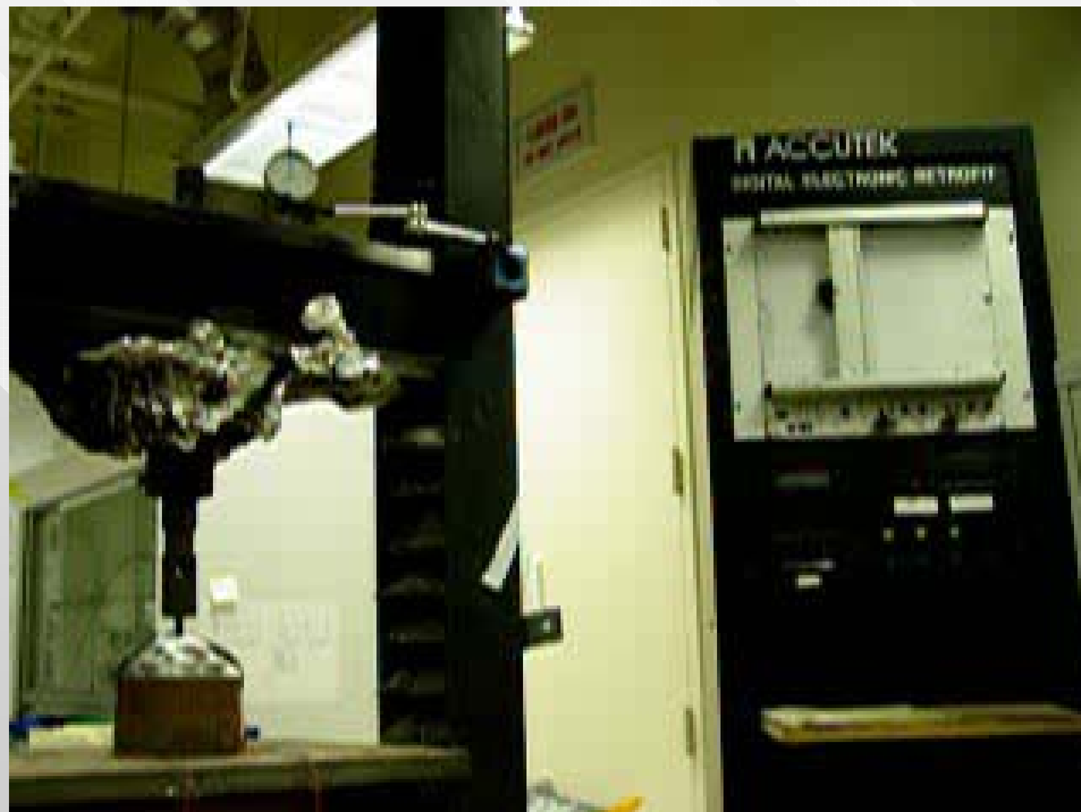

Indentation for Determination of *A* and *m*

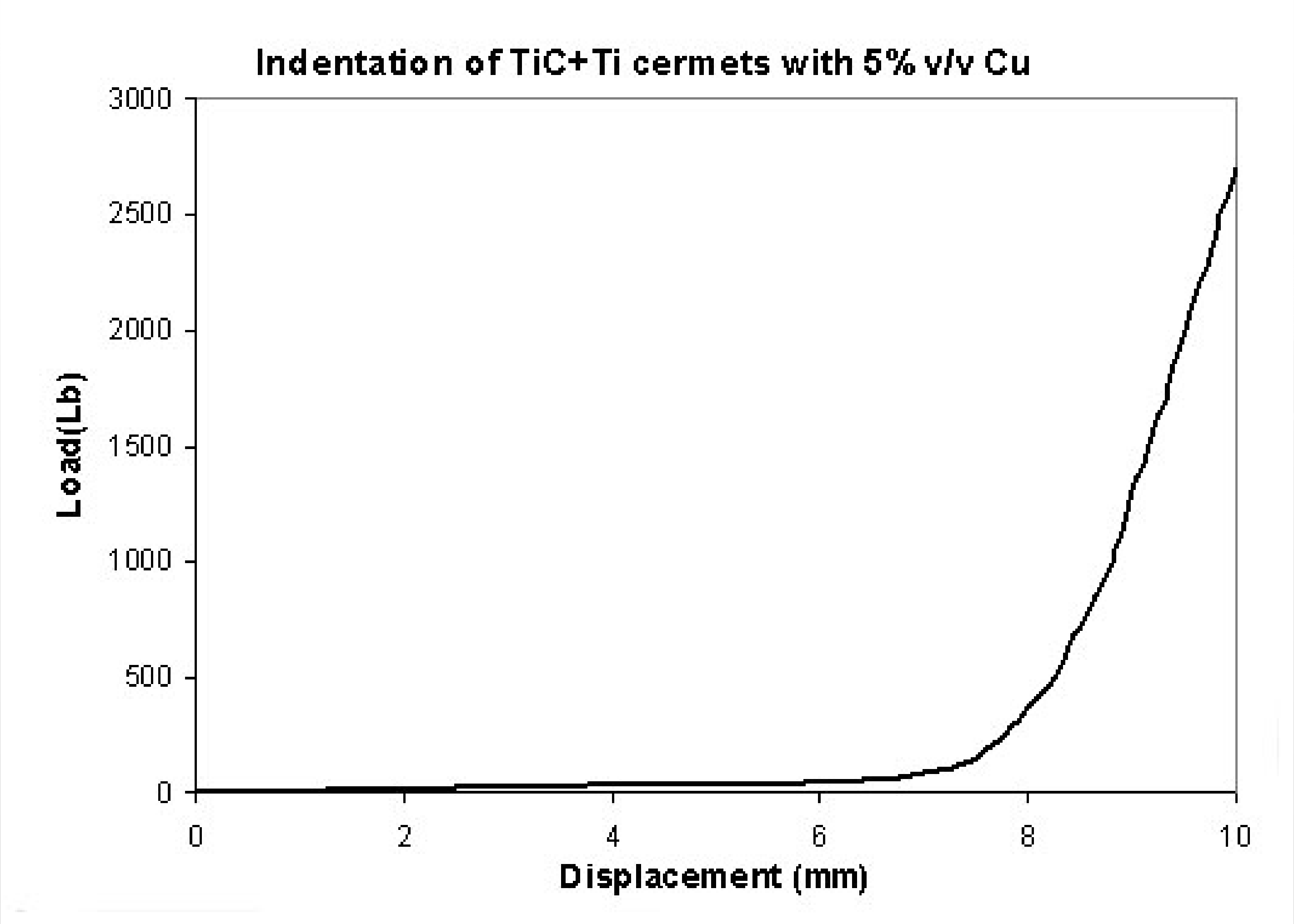

Indentation for Determination of *A* and *m*

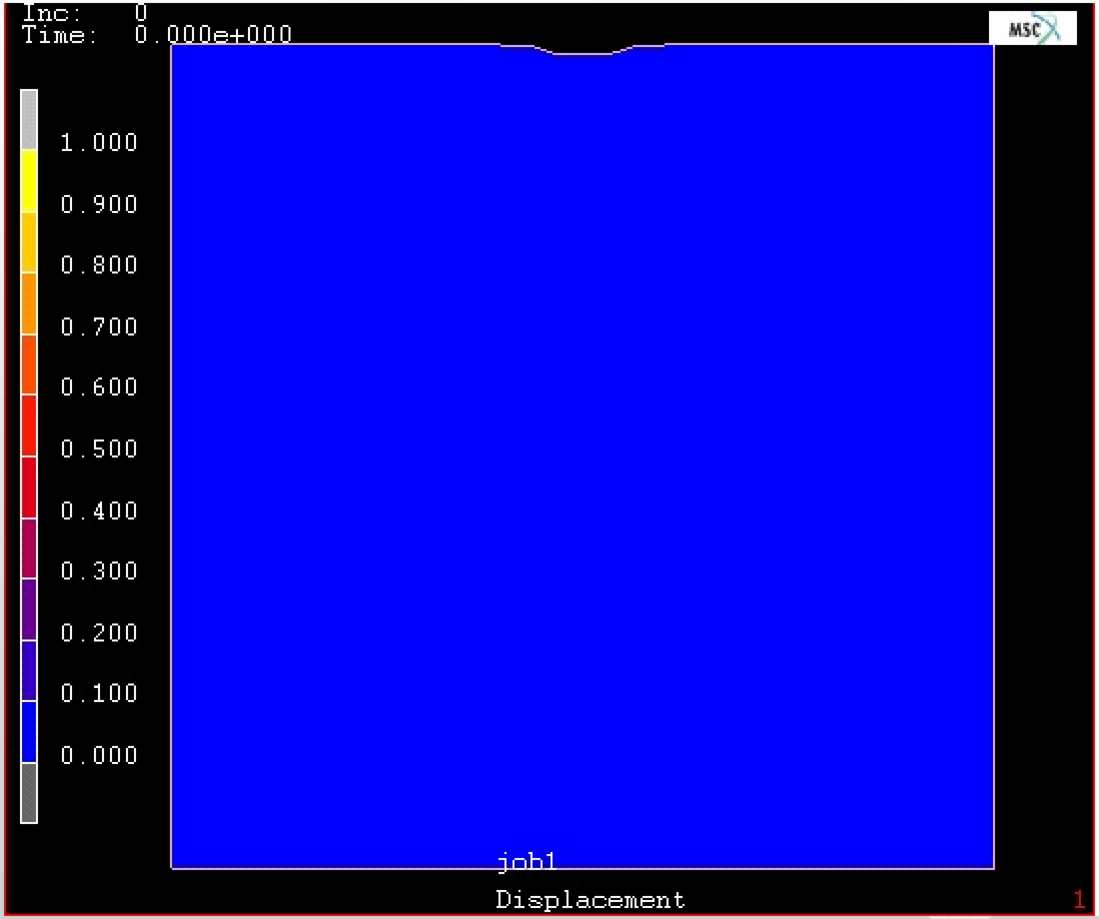

A=110MPa·s$^{0.2}$

m=0.2

Stress-Density Relationship for Power Law creep Models

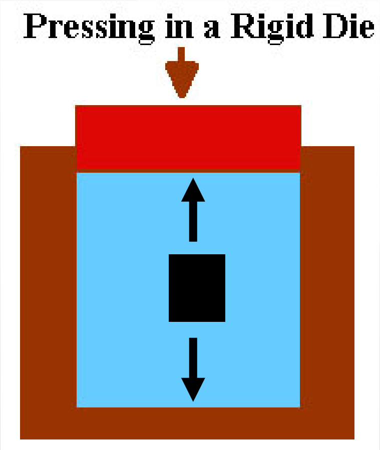

Gurson:

$$\sigma_Z(\rho,T) = -A\left(1-\frac{T-T_0}{T_{am}-T_0}\right)\frac{\left[\frac{4}{27}\frac{\left(1+(1-\rho)^3\right)}{\left(1-(1-\rho)^2\right)}+\frac{2}{9}\frac{\left(1+(1-\rho)^3\right)}{\left(1-(1-\rho)^2\right)(1-\rho)^2}\right]^{\frac{m+1}{2}}}{\rho^{\frac{m-1}{2}}}\dot{\varepsilon}_Z{}^m$$

Skorohod:

$$\sigma_Z(\rho,T) = -A\left(1-\frac{T-T_0}{T_{am}-T_0}\right)\rho^{\frac{m+3}{2}}\left[\frac{2}{3}+\frac{2}{3}\frac{\rho}{(1-\rho)}\right]^{\frac{m+1}{2}}\dot{\varepsilon}_Z{}^m$$

Kuhn&Downey:

$$\sigma_Z(\rho,T) = -A\left(1-\frac{T-T_0}{T_{am}-T_0}\right)\frac{\left[\frac{4}{9\rho\left(2+\rho^2\right)}+\frac{2}{9\rho(1-\rho)(3-\rho)}\right]^{\frac{m+1}{2}}}{\rho^{\frac{m-1}{2}}}\dot{\varepsilon}_Z{}^m$$

McMeeking & Sofronis:

$$\sigma_Z(\rho,T) = -A\left(1-\frac{T-T_0}{T_{am}-T_0}\right)\frac{\left[\frac{2}{3}\left(\frac{\rho}{2-\rho}\right)^{\frac{2}{m+1}}+\frac{2}{3}\left(\frac{1-(1-\rho)^m}{m(1-\rho)^m}\right)^{\frac{2}{m+1}}\right]^{\frac{m+1}{2}}}{\rho^{\frac{m-1}{2}}}\dot{\varepsilon}_Z{}^m$$

Where m is the stain rate sensitivity. A plays the role of a yield stress of a fully-dense material as in Rigid-Plastic models

Comparison of the constitutive models for axial strain compression of hot porous materials and the corresponding experimental curve.

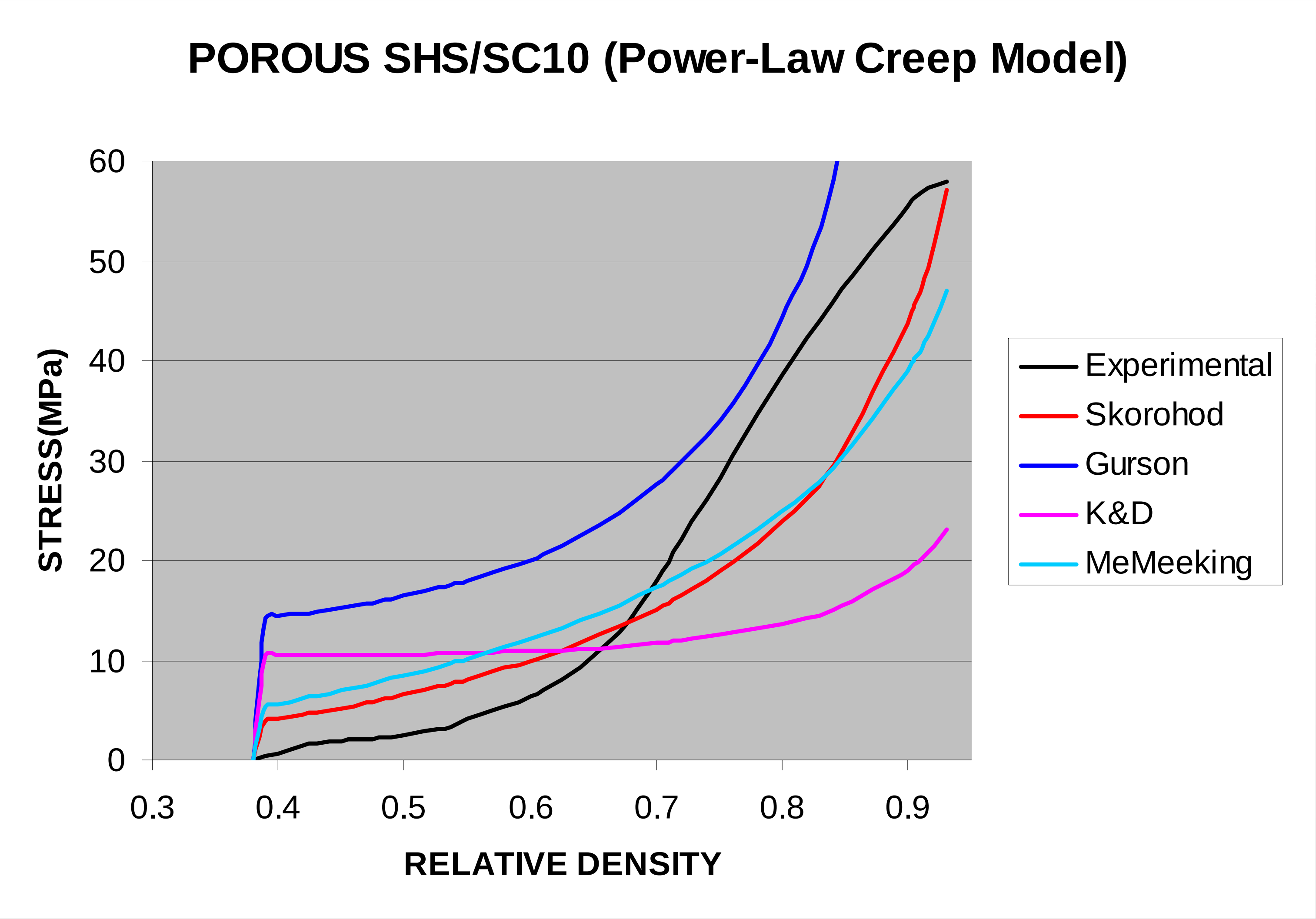

Comparison of the constitutive model for axial strain compression of hot porous TiB_2-Al_20_3 and the corresponding experimental curve.

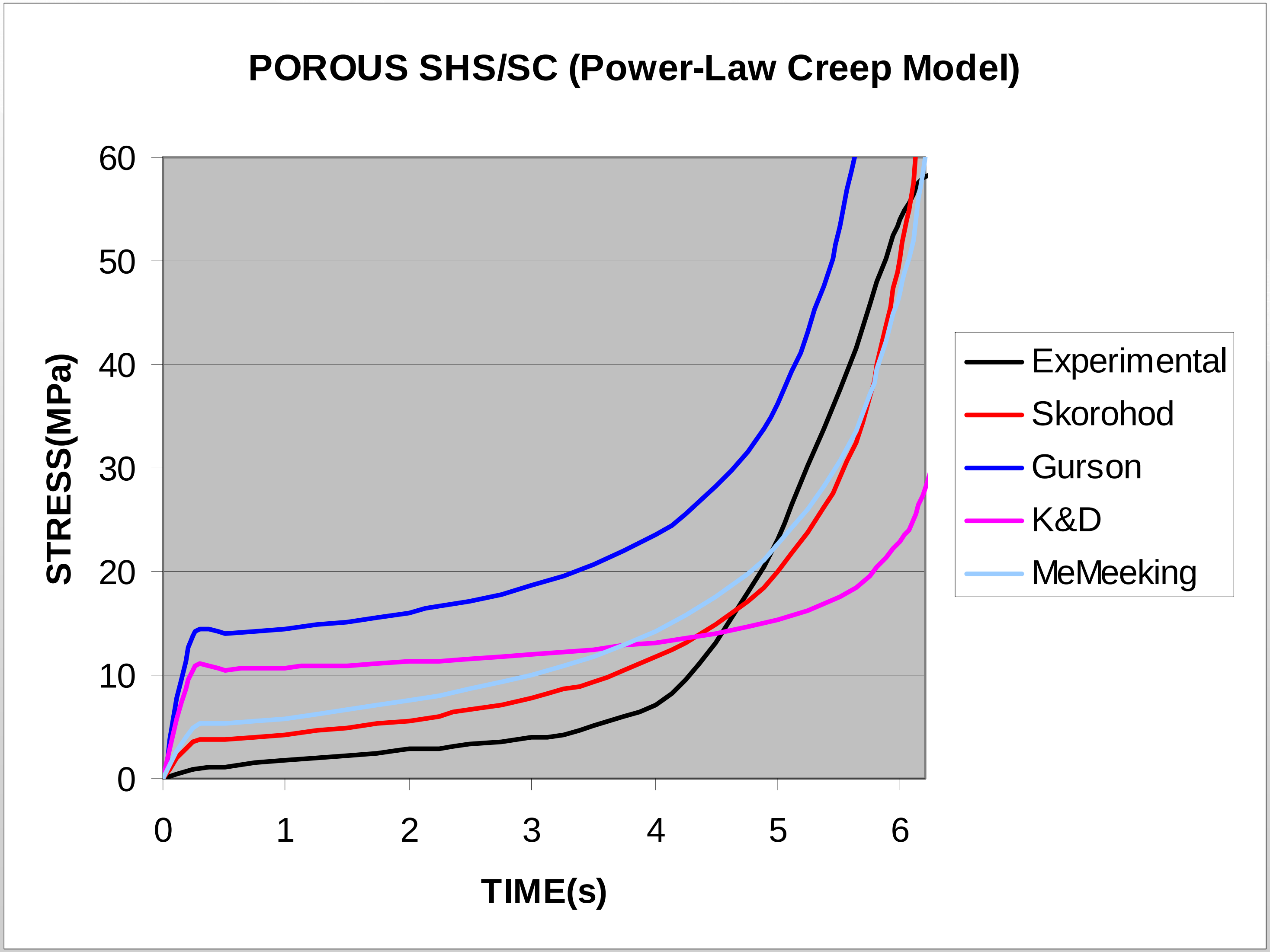

Conclusions on Cermets High Temperature Constitutive Behavior

The best model to use is power-law creep with Skorohod viscosity moduli.

$$\varphi = \frac{1}{\rho^2}$$

$$\psi = \frac{3}{2}\frac{\left(1-\rho\right)}{\rho^3}$$

Cracking of Graphite Particles in PTM

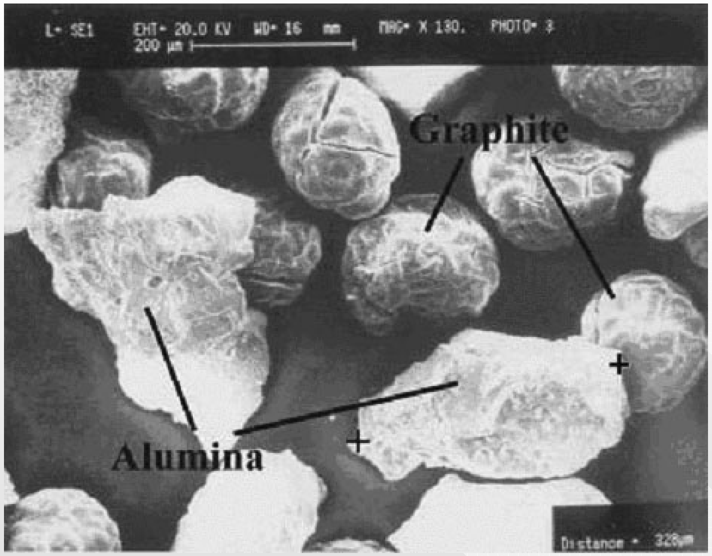

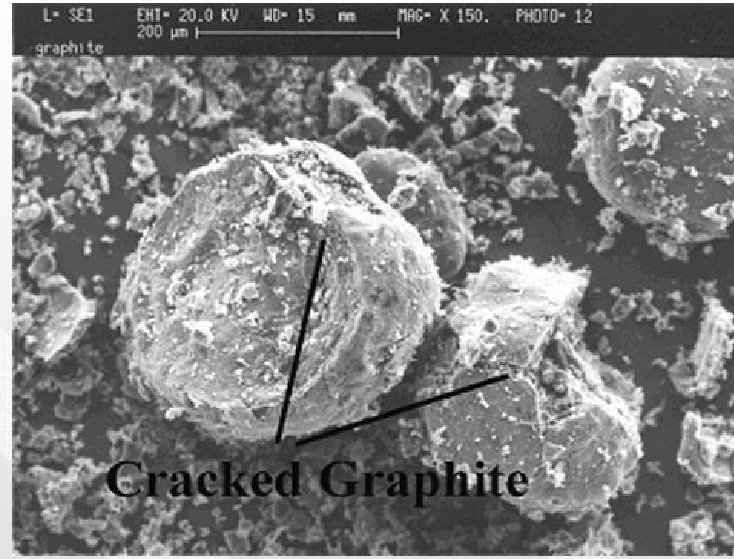

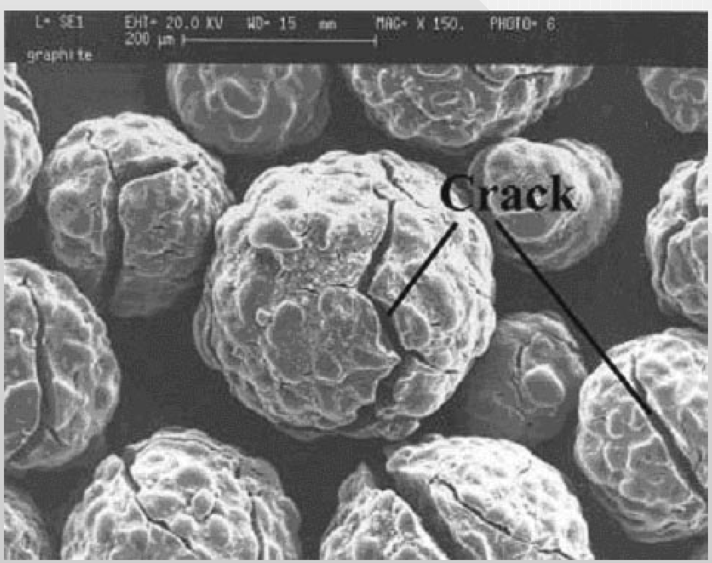

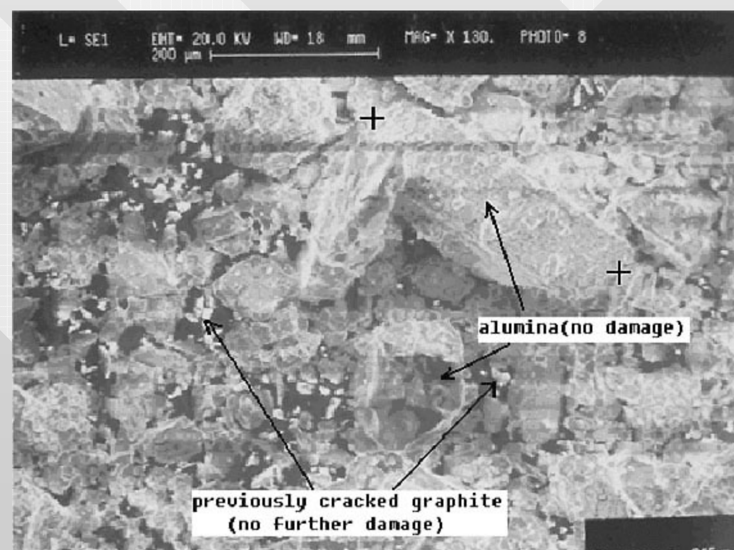

Compression Test of PTM

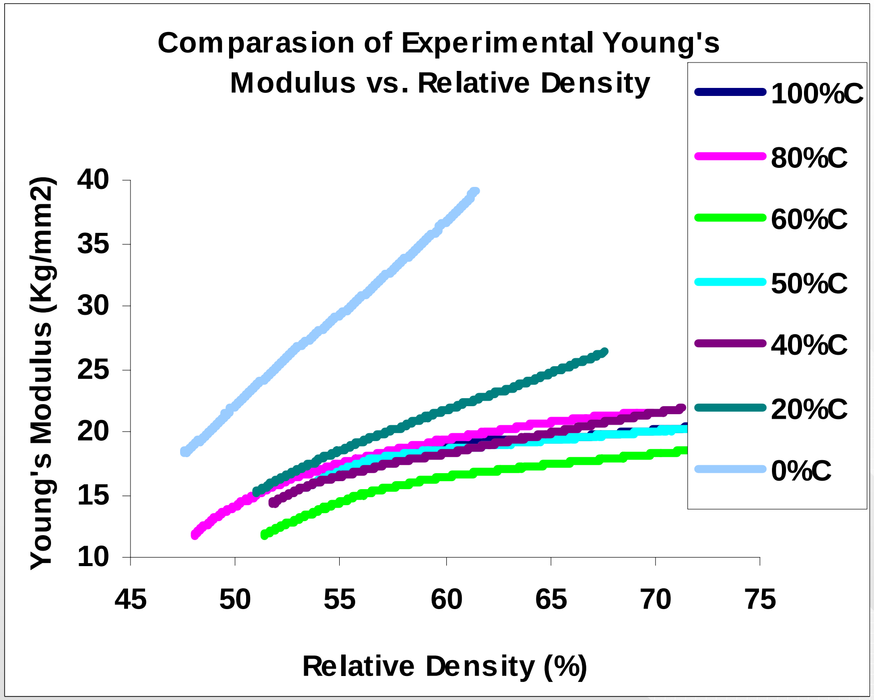

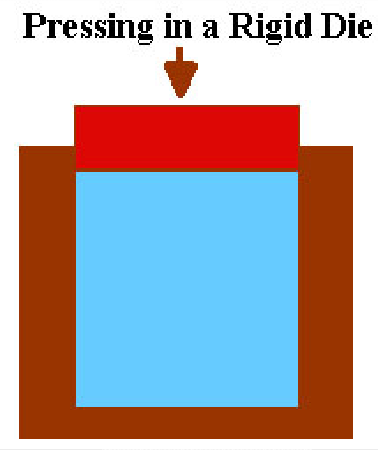

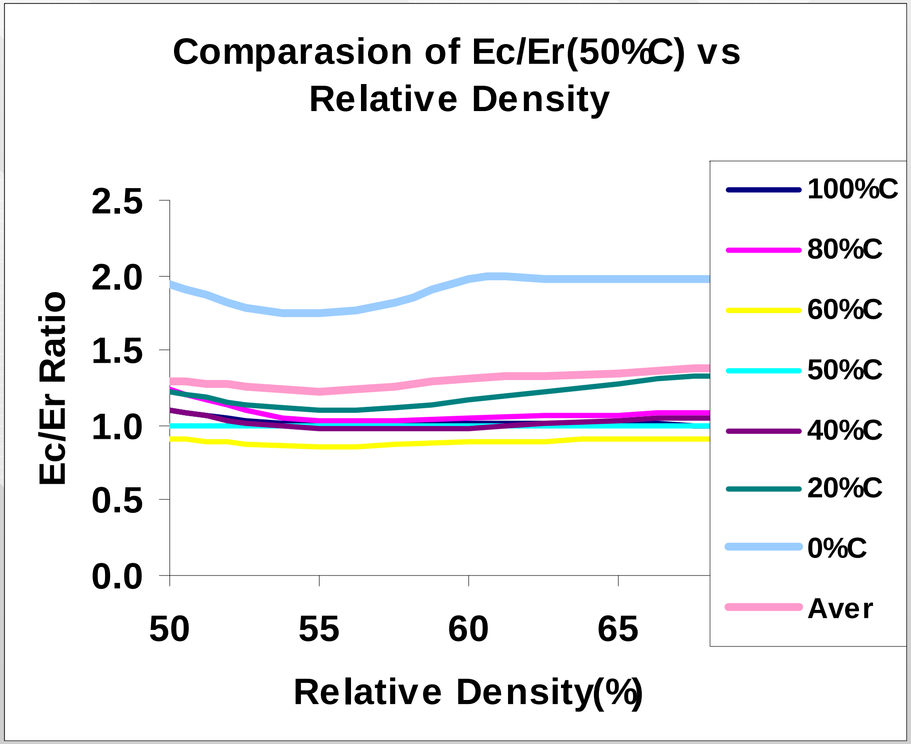

Elastic modeling of PTM

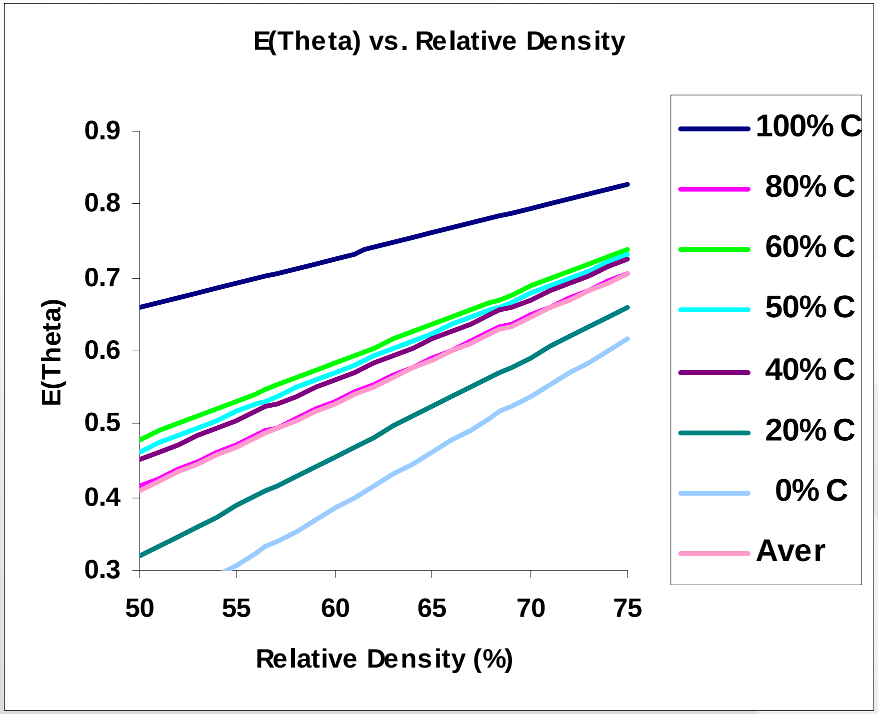

$$E(C,\rho) = E_C \cdot E_{\rho_P}$$

$$E_C = 95.7854 \cdot (C+1)^{-0.27281}$$

$$E_{\rho_P} = (0.0118 \cdot \rho_p - 0.1794)$$

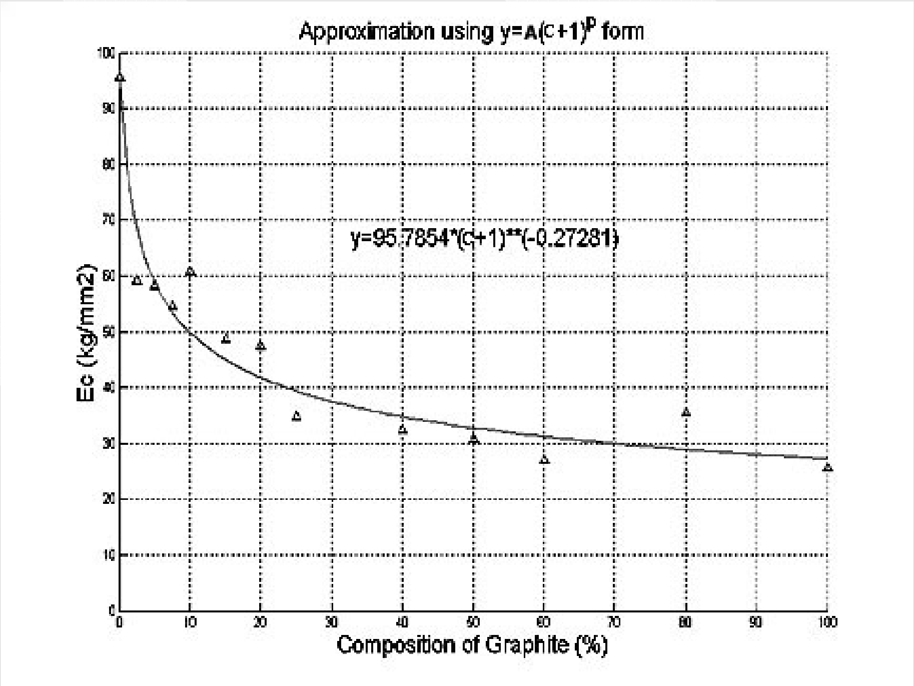

First approximation and possible analytical optimization.

Modeling of QIP

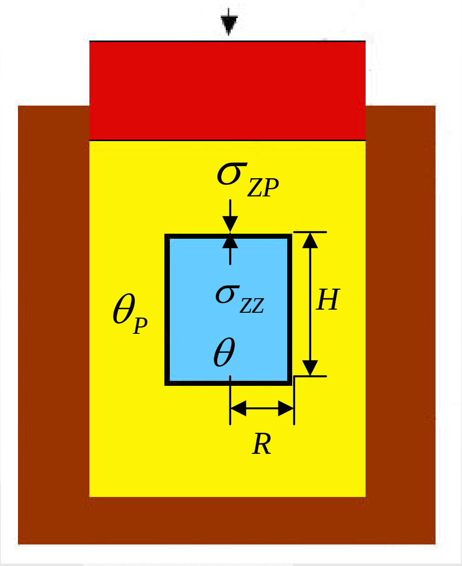

Based on the fact that:

$$\sigma_{ZP} = \sigma_{ZZ}$$

And the constitutive modeling of PTM as well as our former study one have:

$$\frac{d\theta}{d\tau} = -(1-\theta)\left[\frac{143.68}{E_0}(C+1)^{(-0.27281)}\left(0.0118(1-\theta_P)-0.1794\right)\right]^{\frac{1}{m}} \times$$

$$\left[\frac{(4-3\theta_P)}{9\theta_P(1-\theta_P)}\ln\left(\frac{1-\theta_P}{1-\theta_{P0}}\right)\frac{(2-\theta_P)}{(2-3\theta_P)}\frac{\theta}{(1-\theta)^3}\right]^{\frac{1}{m}}\left[\frac{\sqrt{6}(1-\theta)\sqrt{\theta_p{}^2(1-\theta)+\theta(1-\theta_P)^2}}{\theta(4-3\theta_P)}\right]^{\frac{1-m}{m}}$$

$$\tau = \left(\frac{A}{E_0}\right)^{\frac{1}{m}} t$$ **Normalized time (t is physical time)**

Modeling of QIP (continue I)

From the geometry relationships:

$$\frac{d\left(H/H_0\right)}{d\tau}=\frac{H}{3H_0}\left[\frac{2\theta_P+\left(1-3\theta_P\right)\theta}{\theta\left(1-\theta\right)\left(1-\theta_P\right)}\right]\frac{d\theta}{d\tau}$$

$$\frac{d\left(R/R_0\right)}{d\tau}=\frac{R}{3R_0}\left[\frac{\theta-\theta_P}{\theta\left(1-\theta\right)\left(1-\theta_P\right)}\right]\frac{d\theta}{d\tau}$$

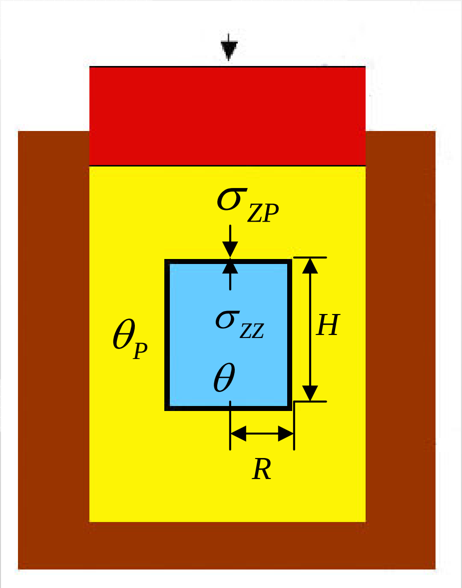

Modeling of QIP (continue II)

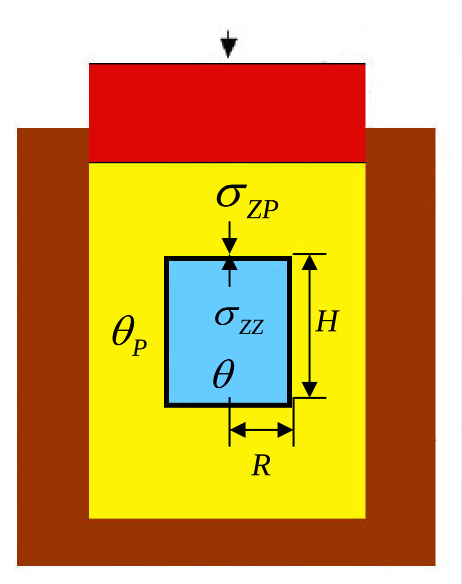

From conservation of mass of the system of PTM + porous cermets:

$$\frac{d\left(\theta_P/\theta_{P_0}\right)}{d\tau}=\frac{\left\{\begin{array}{l}\dfrac{\rho_{Spe}}{\rho_{PTM}}\left[2\dfrac{R}{R_0}\dfrac{H}{H_0}\dfrac{d\left(R/R_0\right)}{d\tau}(1-\theta)+\left(\dfrac{R}{R_0}\right)^2\dfrac{d\left(H/H_0\right)}{d\tau}(1-\theta)-\left(\dfrac{R}{R_0}\right)^2\dfrac{H}{H_0}\dfrac{d\theta}{d\tau}\right]\\ -\left[\left(\dfrac{R_d^0}{R_0}\right)^2\dfrac{\dot{\vartheta}}{H_0}\left(\dfrac{A}{E_0}\right)^{\frac{1}{m}}+2\dfrac{R}{R_0}\dfrac{H}{H_0}\dfrac{d\left(R/R_0\right)}{d\tau}+\left(\dfrac{R}{R_0}\right)^2\dfrac{d\left(H/H_0\right)}{d\tau}\right](1-\theta_P)\end{array}\right\}}{\left[\left(\dfrac{R_d^0}{R_0}\right)^2\left[\dfrac{H_d^0-\dot{\vartheta}\left(A/E_0\right)^{\frac{1}{m}}\tau}{H_0}\right]-\left(\dfrac{R}{R_0}\right)^2\dfrac{H}{H_0}\right]}$$

A sample kinetics of densification, shrinkage and distortion

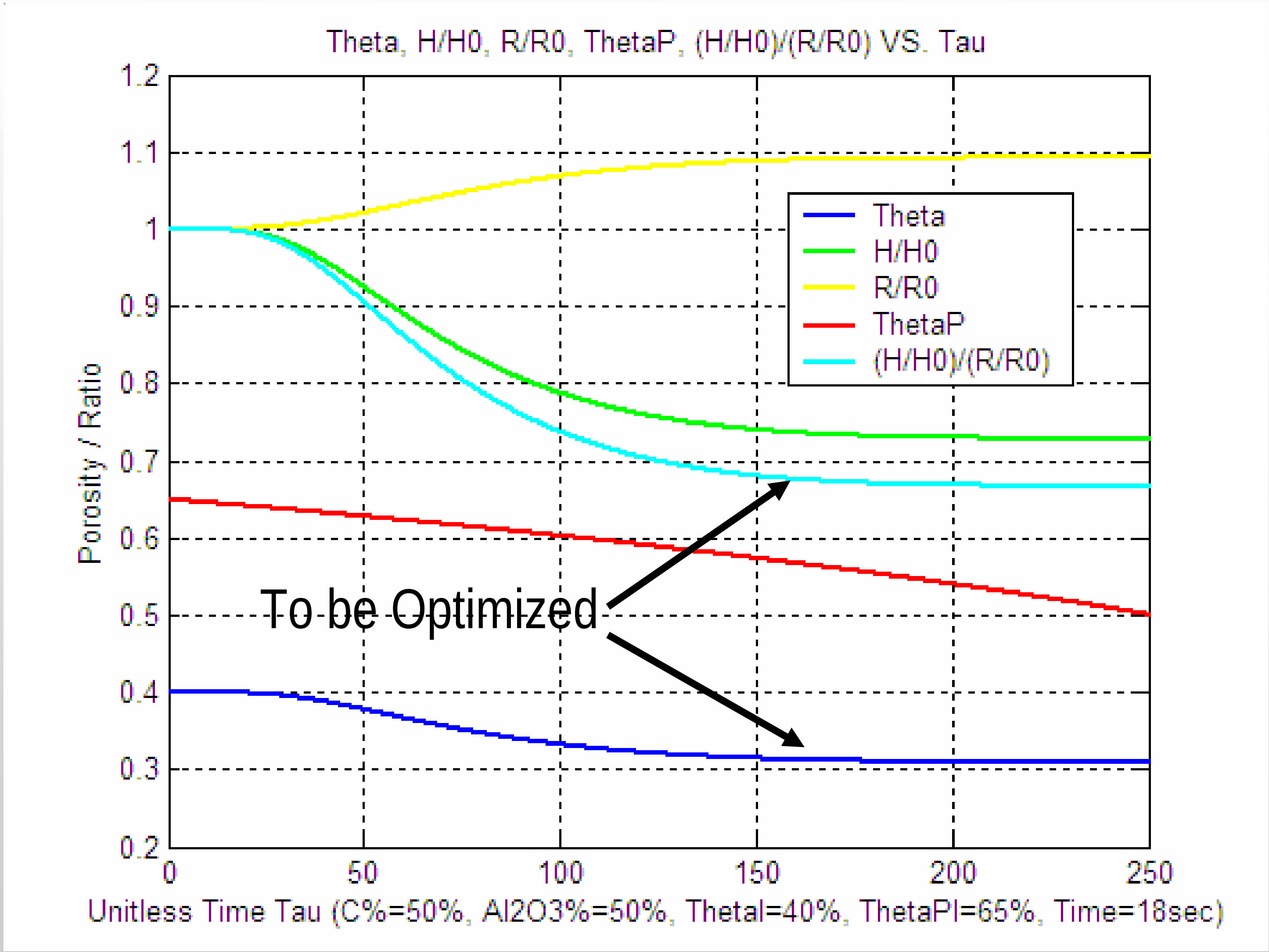

Densification and Distortion Rates

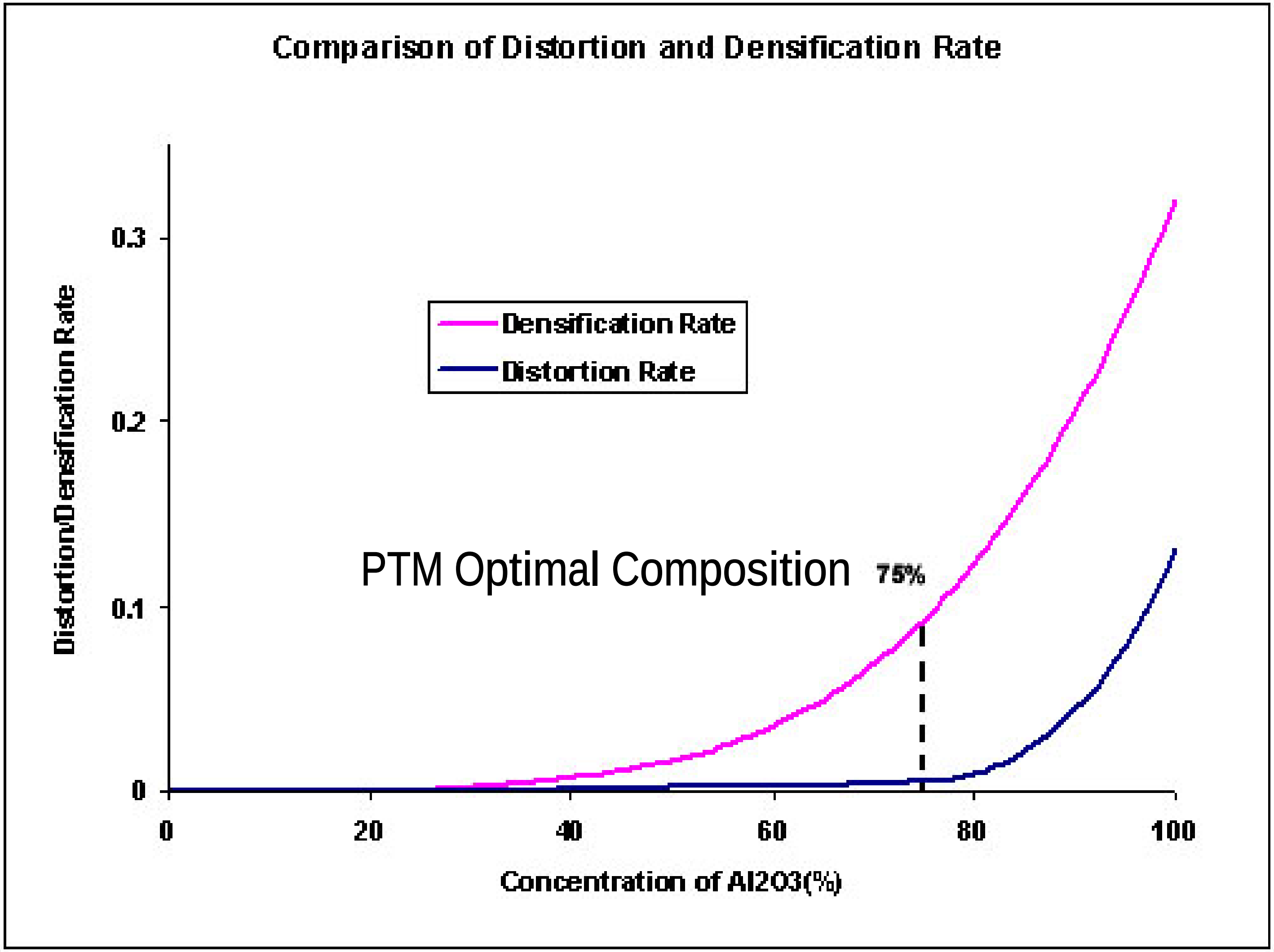

Experiments

Objective and Tasks

- **Determine the "optimal" nonstoichiometric ratio of Ti and C powders for the synthesis of TiC-Ti cermet**

1. Understand mechanical and morphological properties of elemental titanium and graphite powders used in this study.
2. Conduct a series of combustion experiments without densification for different nonstoichiometric ratios of titanium and graphite powders.
3. Determine the optimal nonstoichiometric ratio to be used in further studies.

Objective and Tasks (continue)

- **Determine the time window between combustion and densification and the densification load needed to obtain dense net-shape final products**

1. **Determine the time window between combustion and consolidation in order to obtain dense net-shape final products.**
2. **Determine the load needed to obtain dense net-shape final products.**
3. **Compare the experimental results on shape distortion with theoretical modeling results and make necessary adjustments to the theoretical models.**

Elemental Ti and C Powders

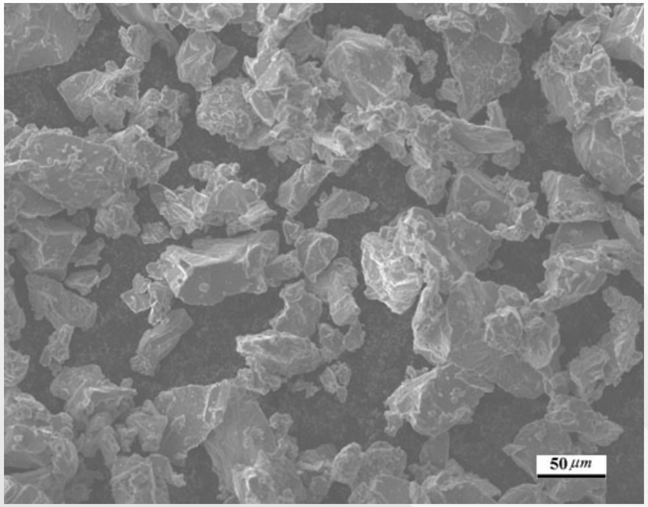

Ti Powder

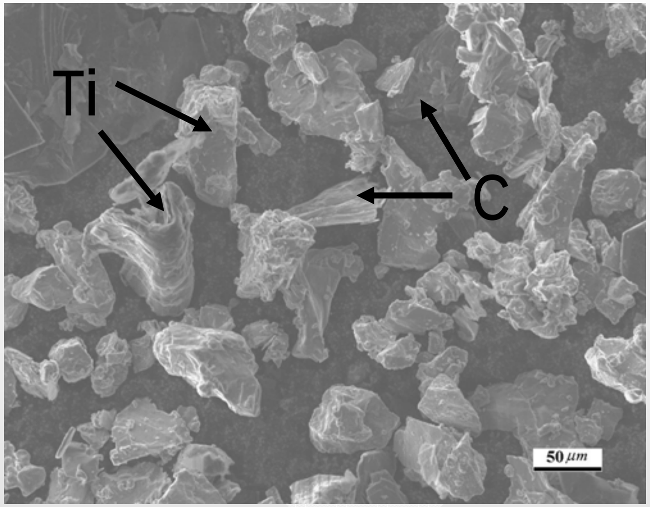

Ti + C Mixture

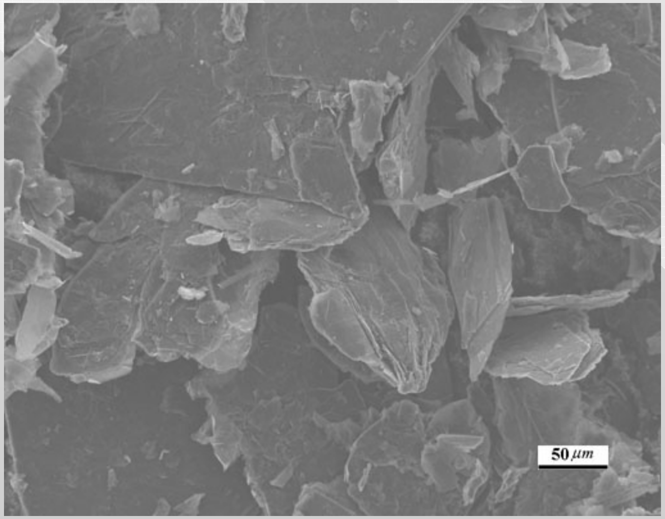

C Powder

Best Nonstoichiometric Ratio

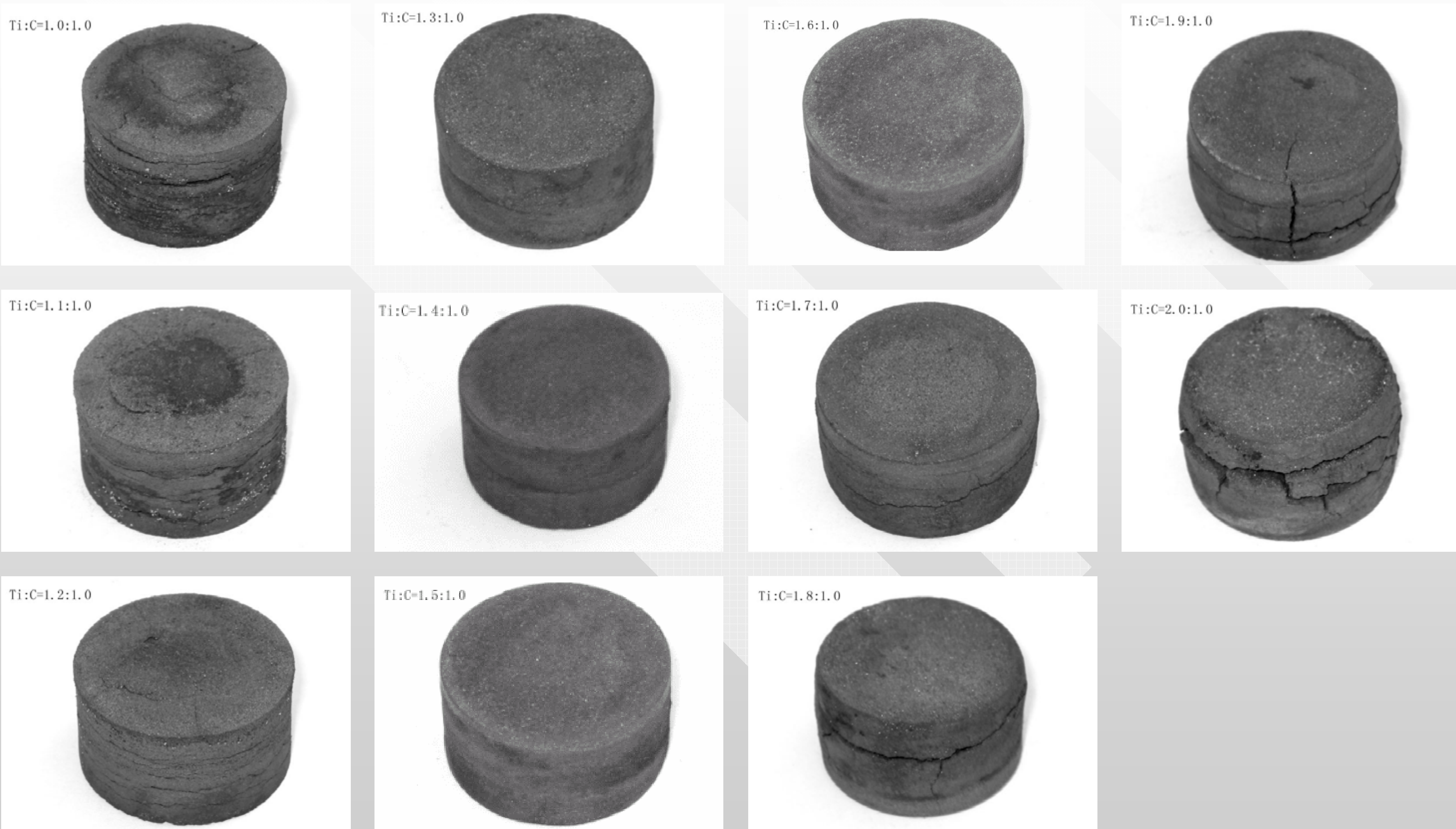

Time Window

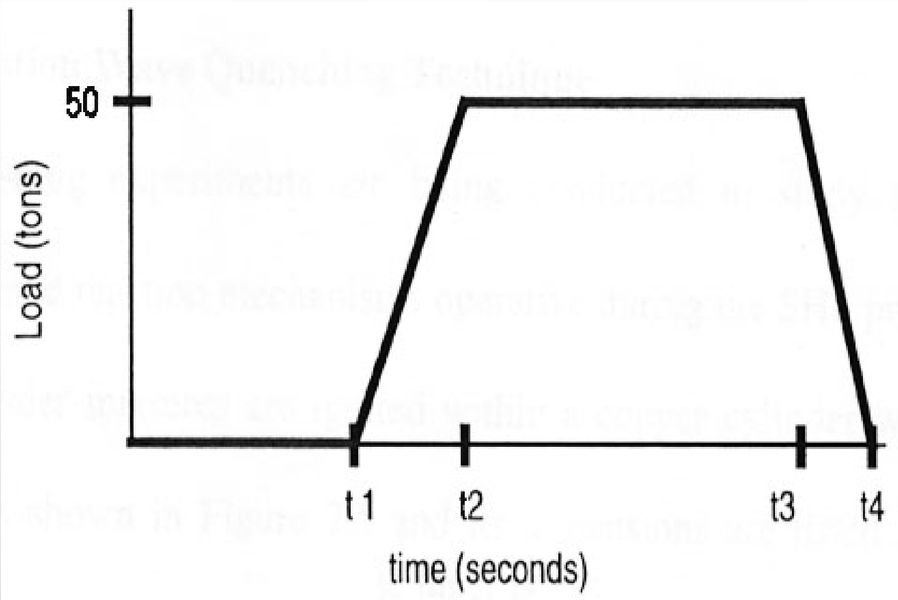

Parameters	Time Zone	Times(s)
Delay	t1	4-5
Loading Time	(t2-t1)	5-10
Holding Time	(t3-t2)	10-15
Unloading Time	(t4-t3)	1-2

Time Window (continue)

Radial cracks caused by excessive delay

Less ductility results in high porosity

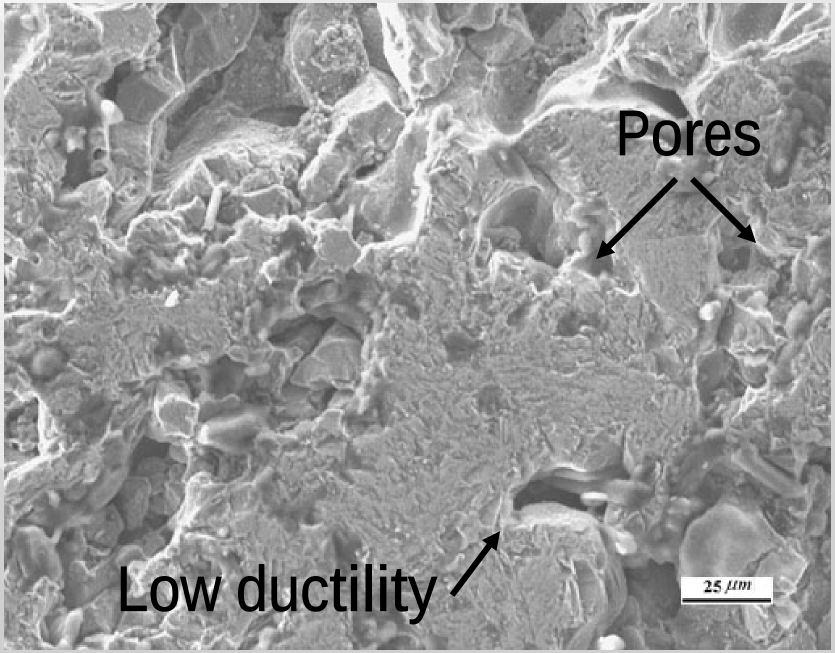

Load Scale

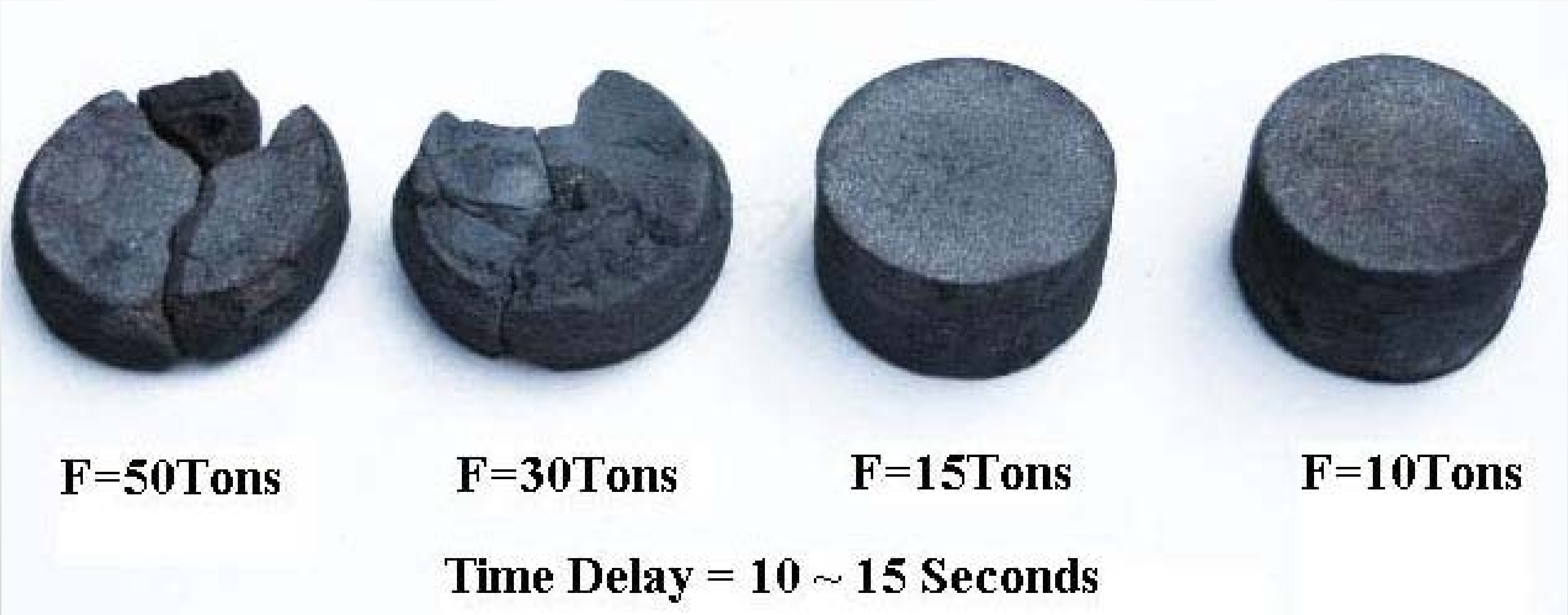

Load is not a critical factor. Based on experiments and former studies, a densification load between 50 Tons and 70 Tons is used for further investigation.

Other Factors

• Influence of C particle size: Small Size -> Excessively Active

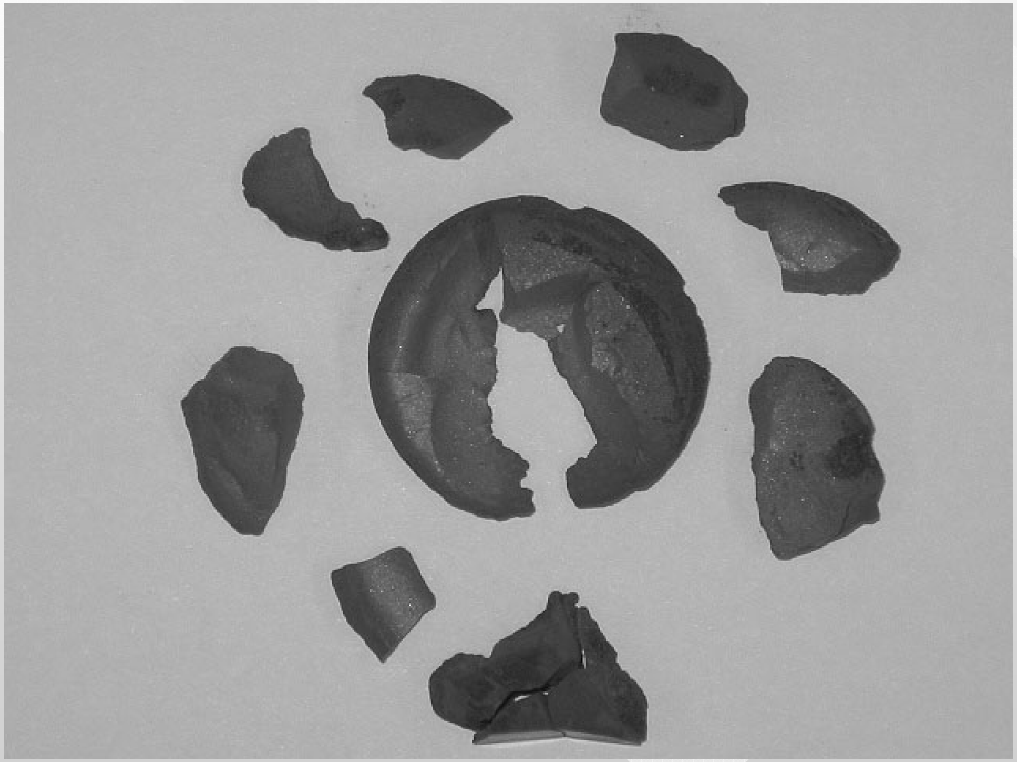

• Influence of low melting temperature metallic binder

Final Product

Finite Element Method Simulation

FEM Simulation Objective and Tasks

- **FEM method to simulate densification of porous materials in QIP setup and optimize initial shape of green sample to get net-shape final products.**

1. Determine material parameters needed to conduct FEM simulation (A, m, Initial Porosity).
2. Develop an FEM simulation of QIP based on the theory of nonlinear-viscous porous bodies (by E.A. Olevsky and A. Maximenko).
3. Conduct FEM simulation of QIP using Mohr-Coulomb and Drucker-Prager models of the commercial FEM package ABAQUS for PTM.
4. Optimize initial shape of a green sample in order to obtain high-density net-shape final products of SHS-QIP technological sequence.

Theory of Plastic Porous Materials

If energy dissipation in the material depends only on the strain rate tensor components: (*D* is average dissipation rate density)

$$\Phi = \int_0^1 D(\alpha \dot{e}, \alpha \dot{\gamma}) \frac{d\alpha}{\alpha}$$

The dissipation potential is the main component in the extremum principle for the kinematic parameters of deformation. It was proved that velocities of a real deformation process render the minimum for the following functional:

$$I = \int_\Omega \Phi d\Omega - \int_\Omega F \cdot v d\Omega - \int_S T \cdot v dS$$

In minimization of *I*, the following approximation of *D* was used in iterative method of viscous approximations

$$D \approx D_v = \sigma_0 \dot{\varepsilon}_0{}^{-m} \sqrt{1-\theta}\, \frac{\psi \dot{e}^2 + \varphi \dot{\gamma}^2}{(\psi \dot{e}_0{}^2 + \varphi \dot{\gamma}_0{}^2)^{\frac{1-m}{2}}}$$

Schematic Representation of QIP Setup

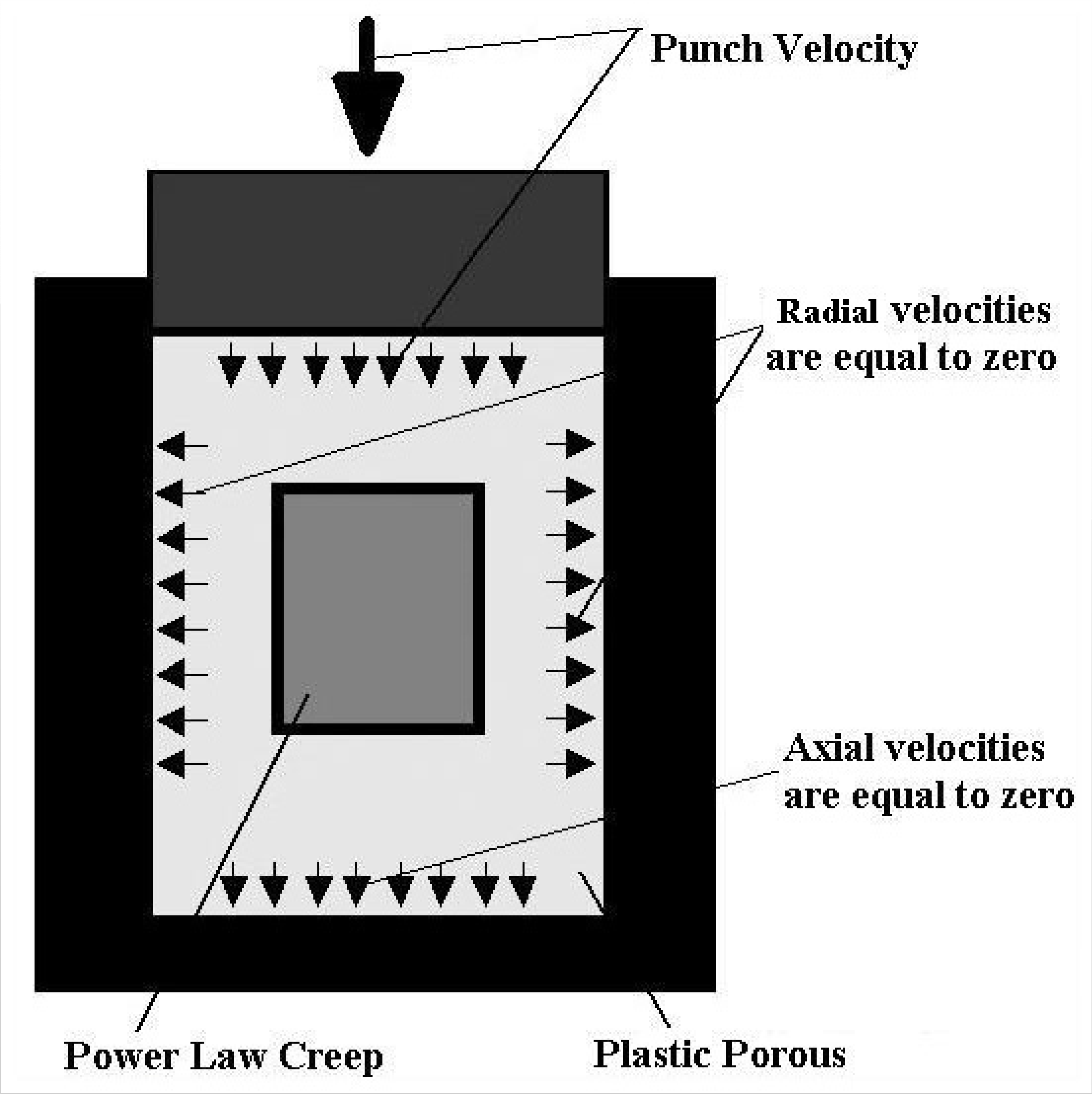

Finite Element Model

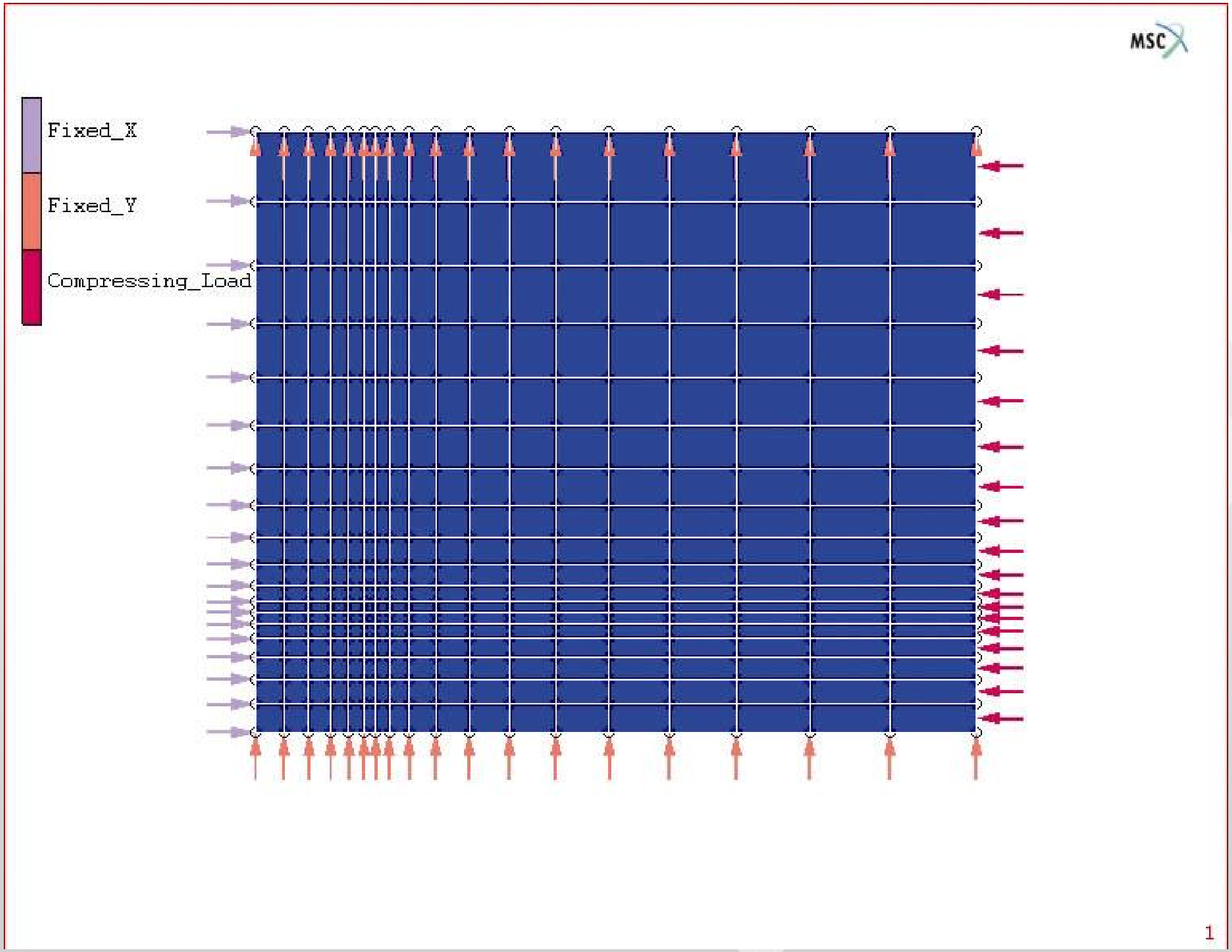

Mesh and Boundary conditions

Finite Element Model (continue I)

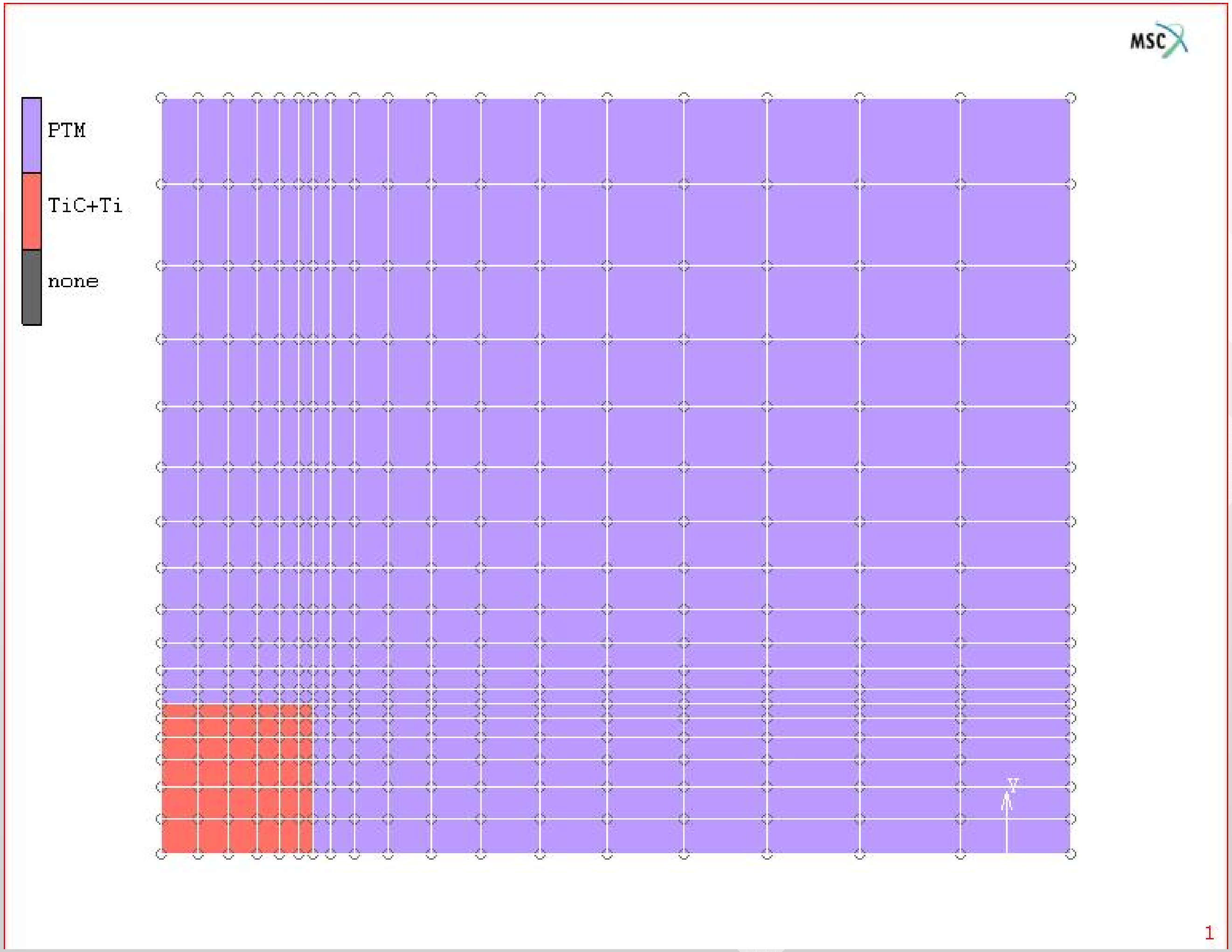

Material properties

Finite Element Model (continue II)

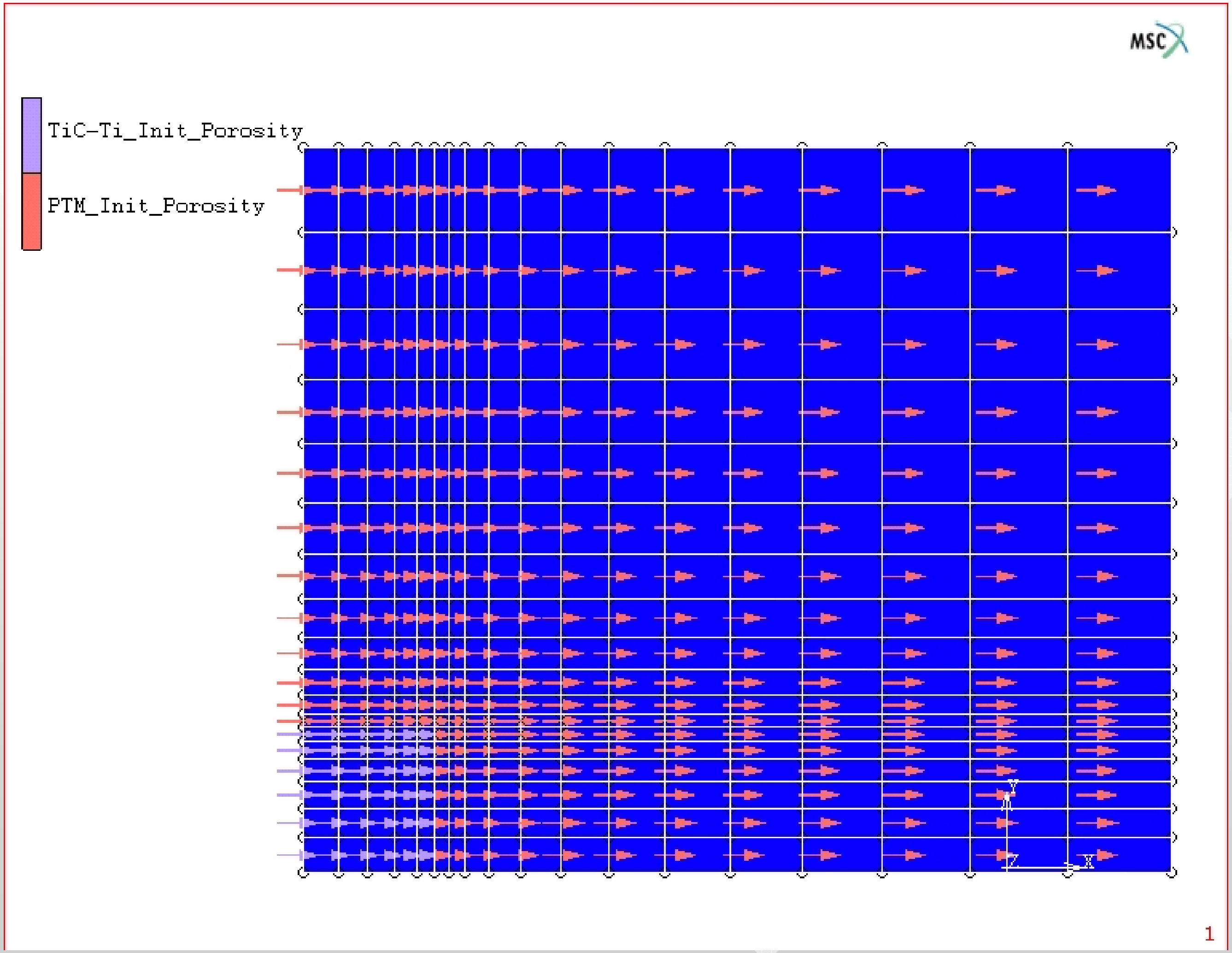

Initial conditions

FEM Results (Nonlinear-Viscous Porous Theory)

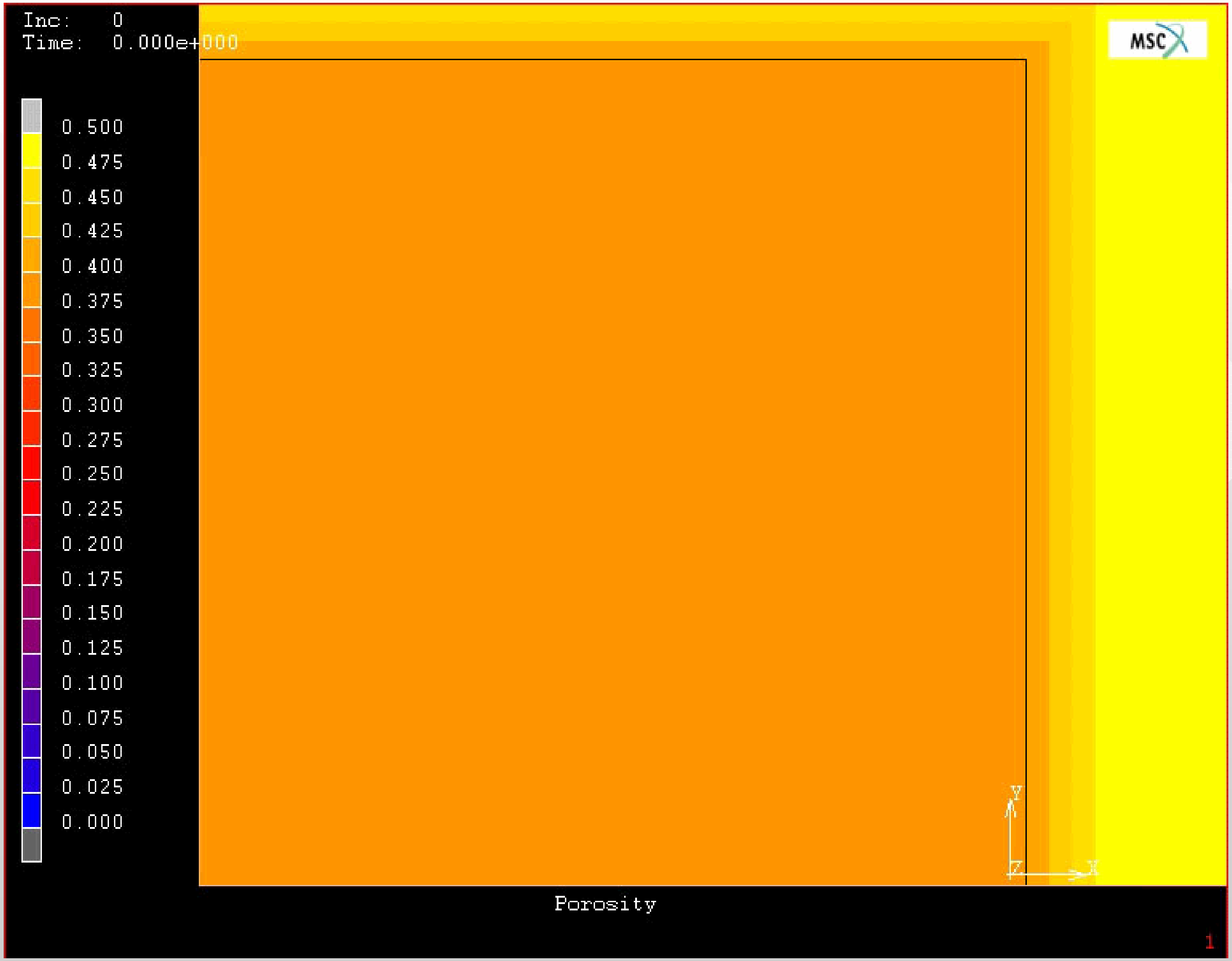

Determination of q_1,q_2 and q_3 for Tvergaard-Gurson Model

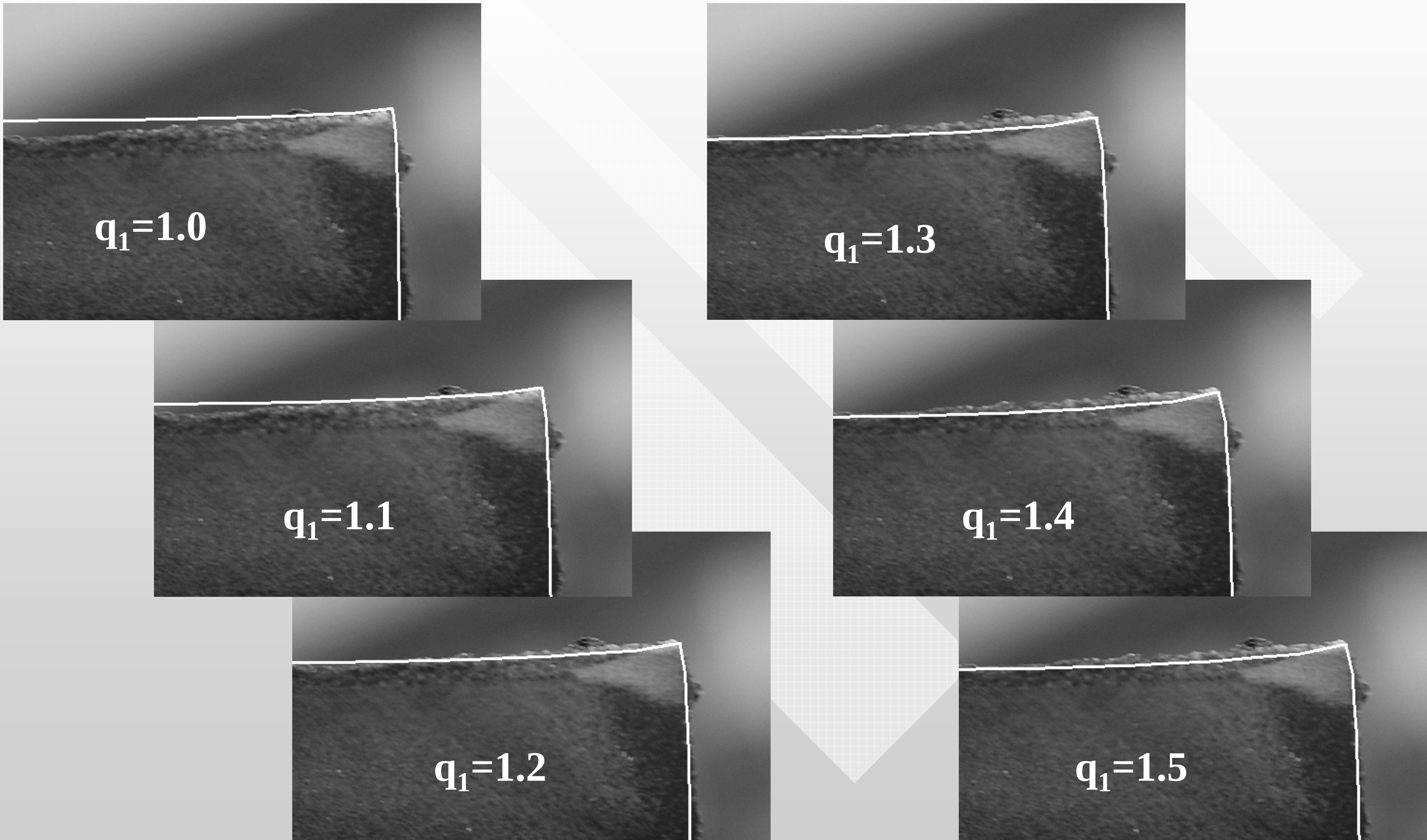

FEM Results (Mohr-Coulomb Model)

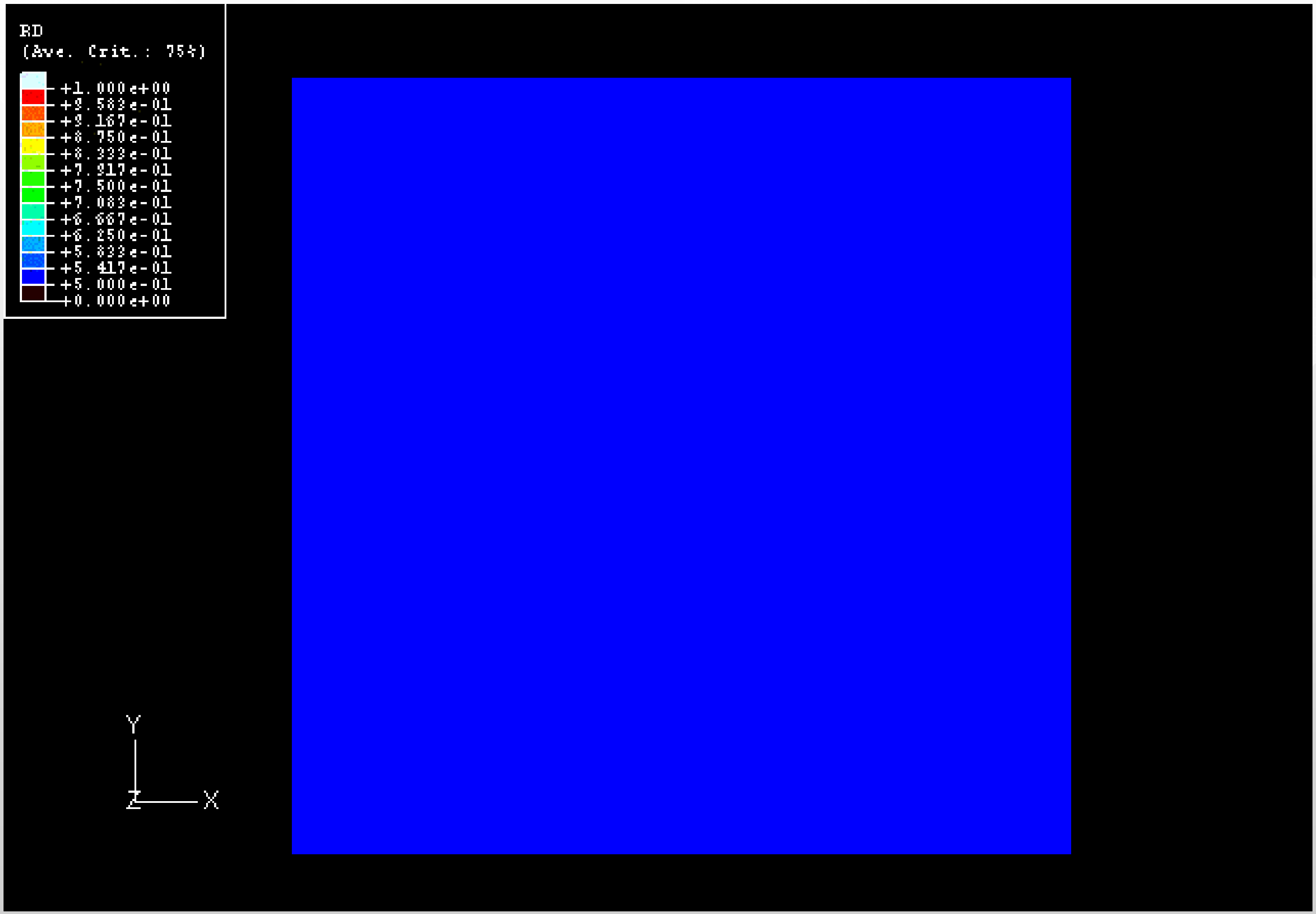

FEM Results (Drucker-Prager/Cap Model)

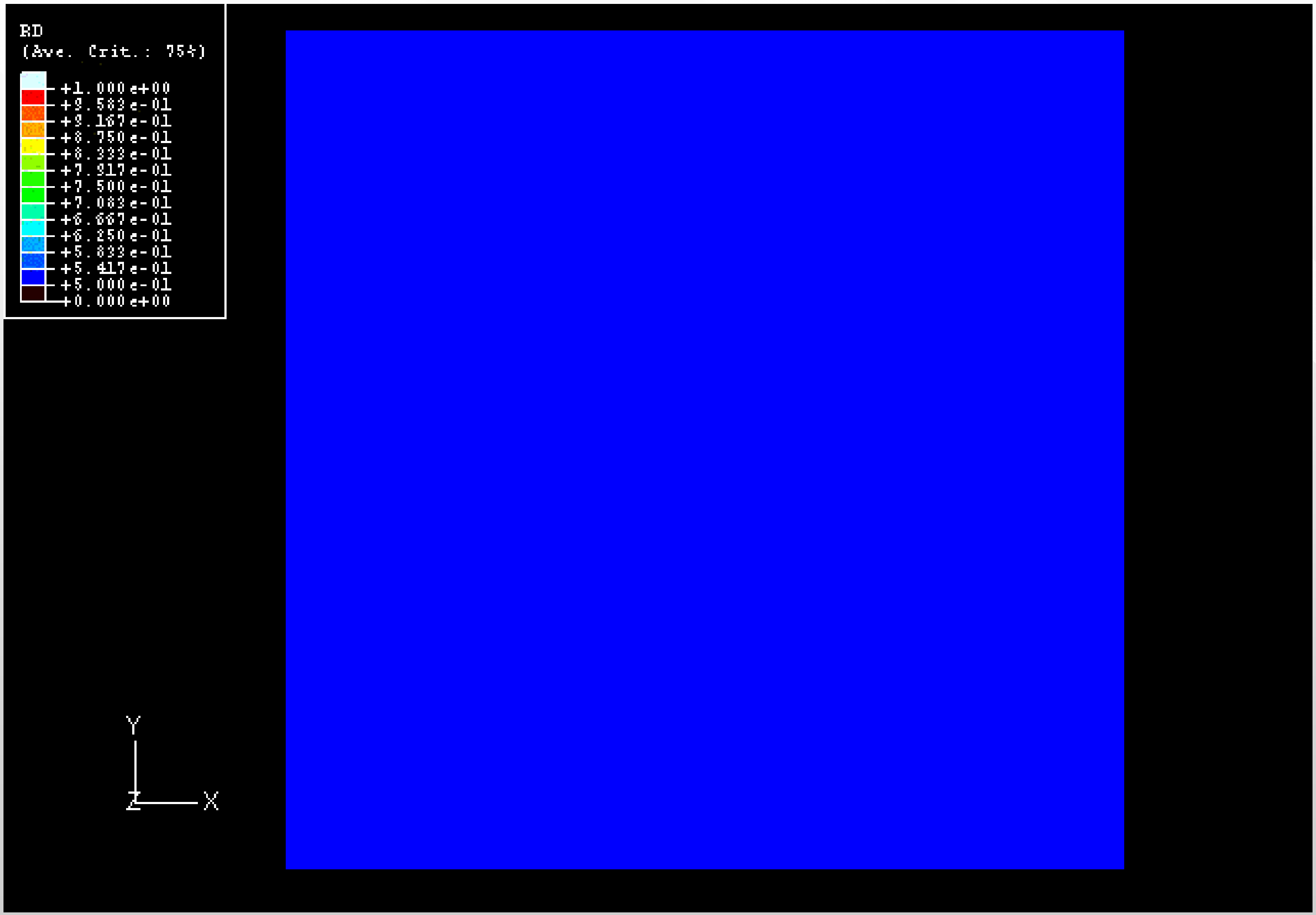

FEM Results (Drucker-Prager/Cap 3D Model)

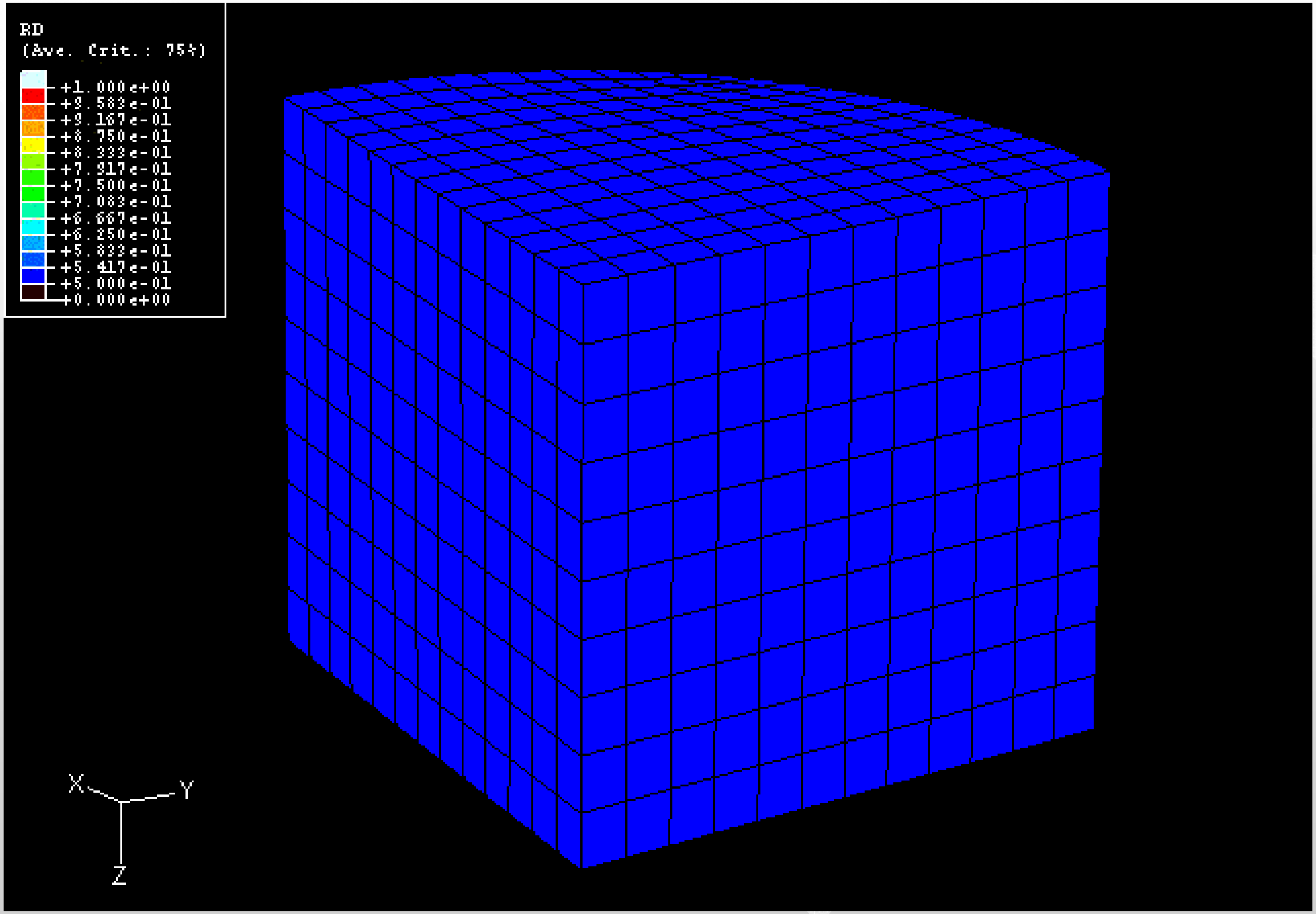

Comparison of the Results of the Three Models

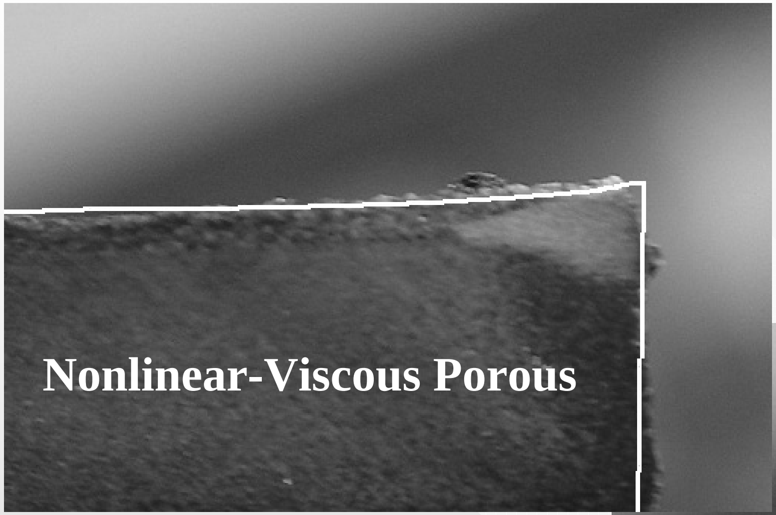

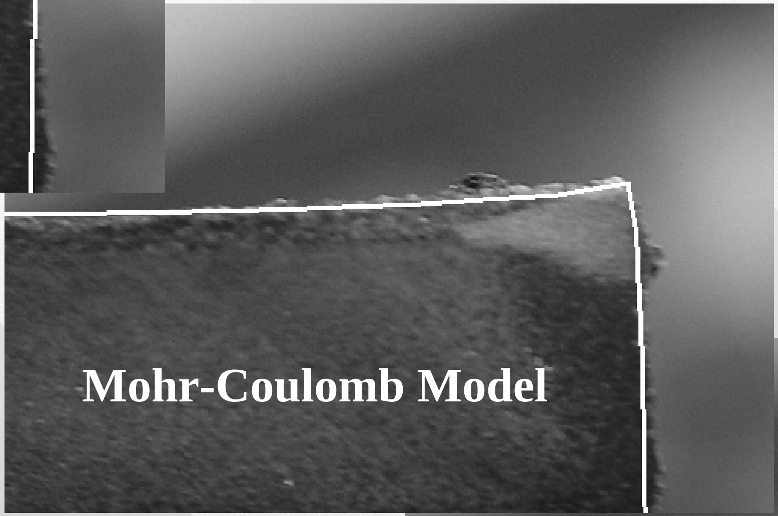

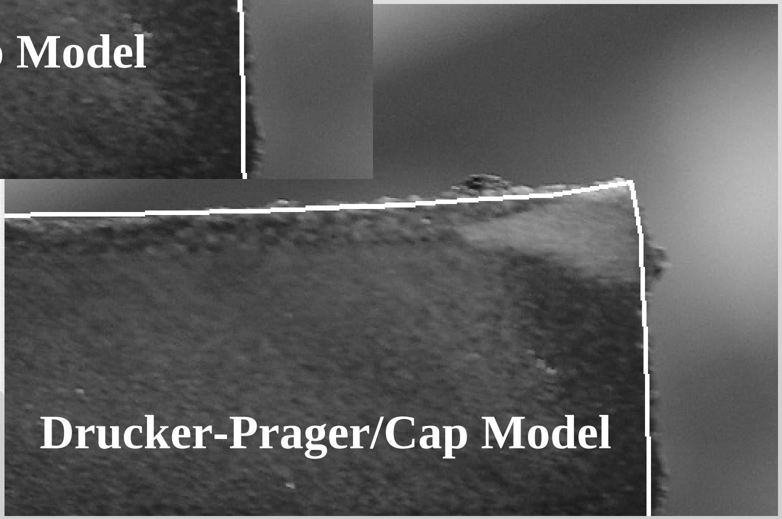

Comparison of Distortion Aspect Ratio

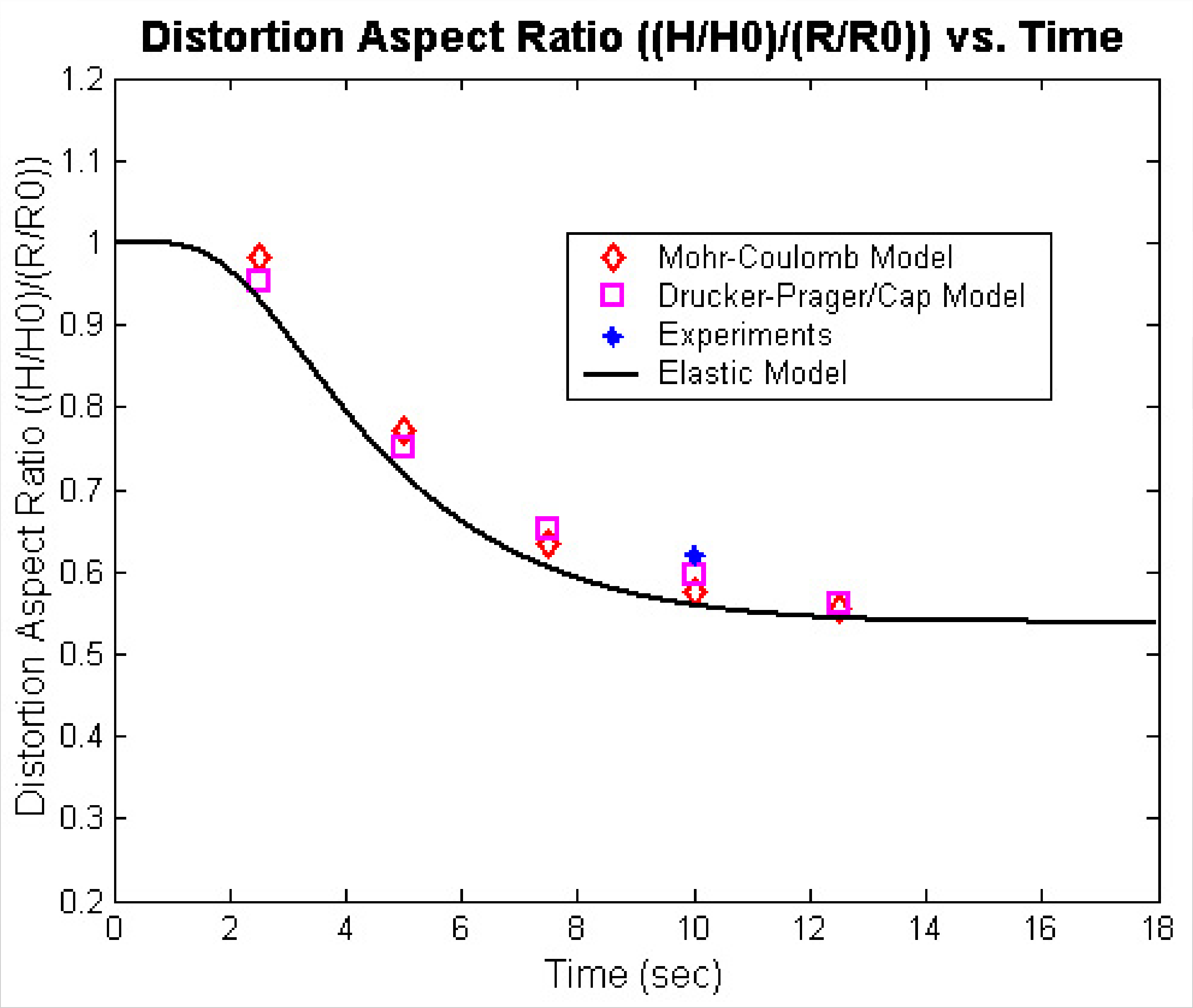

Optimization of Initial Shape

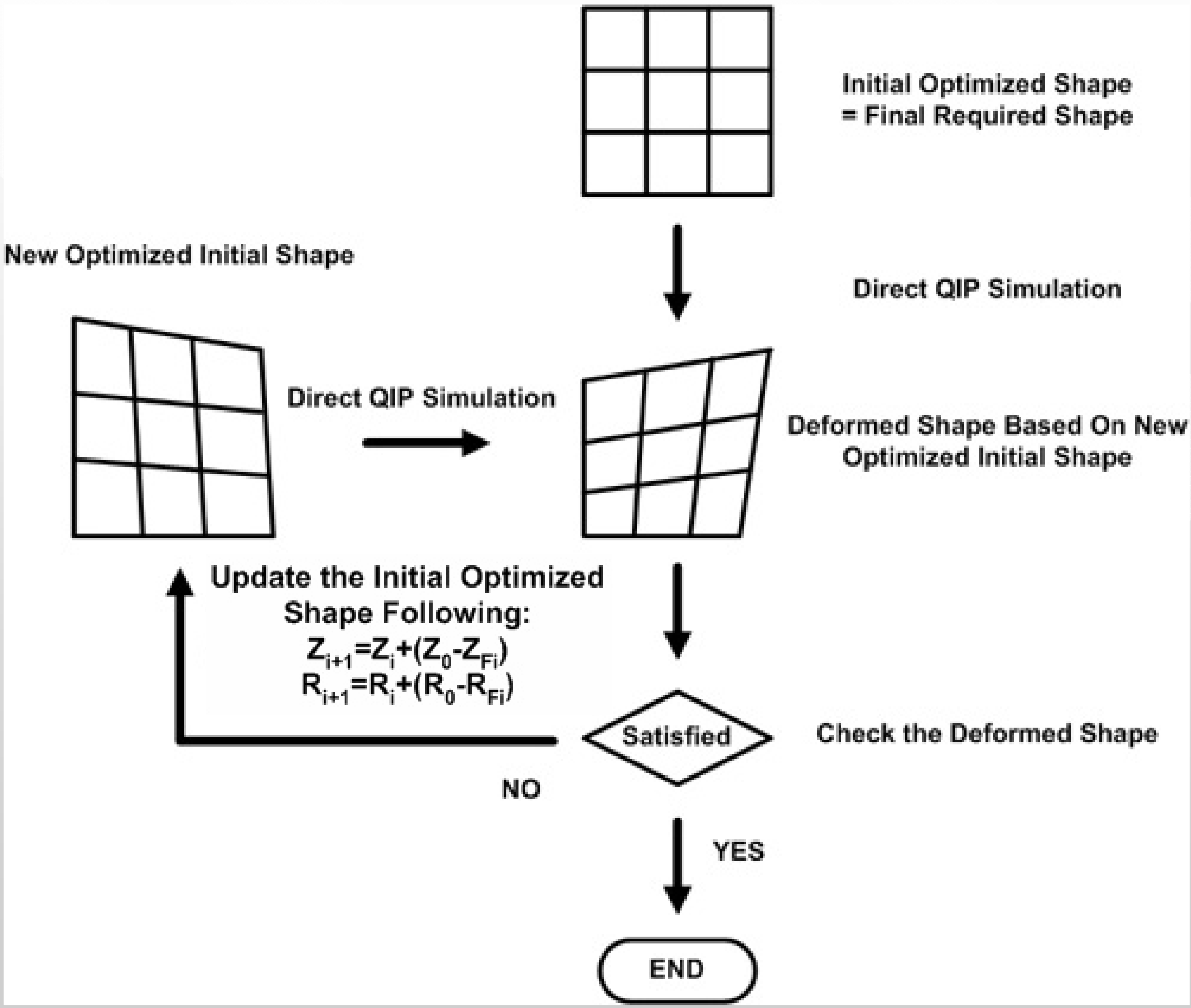

Optimization of Initial Shape

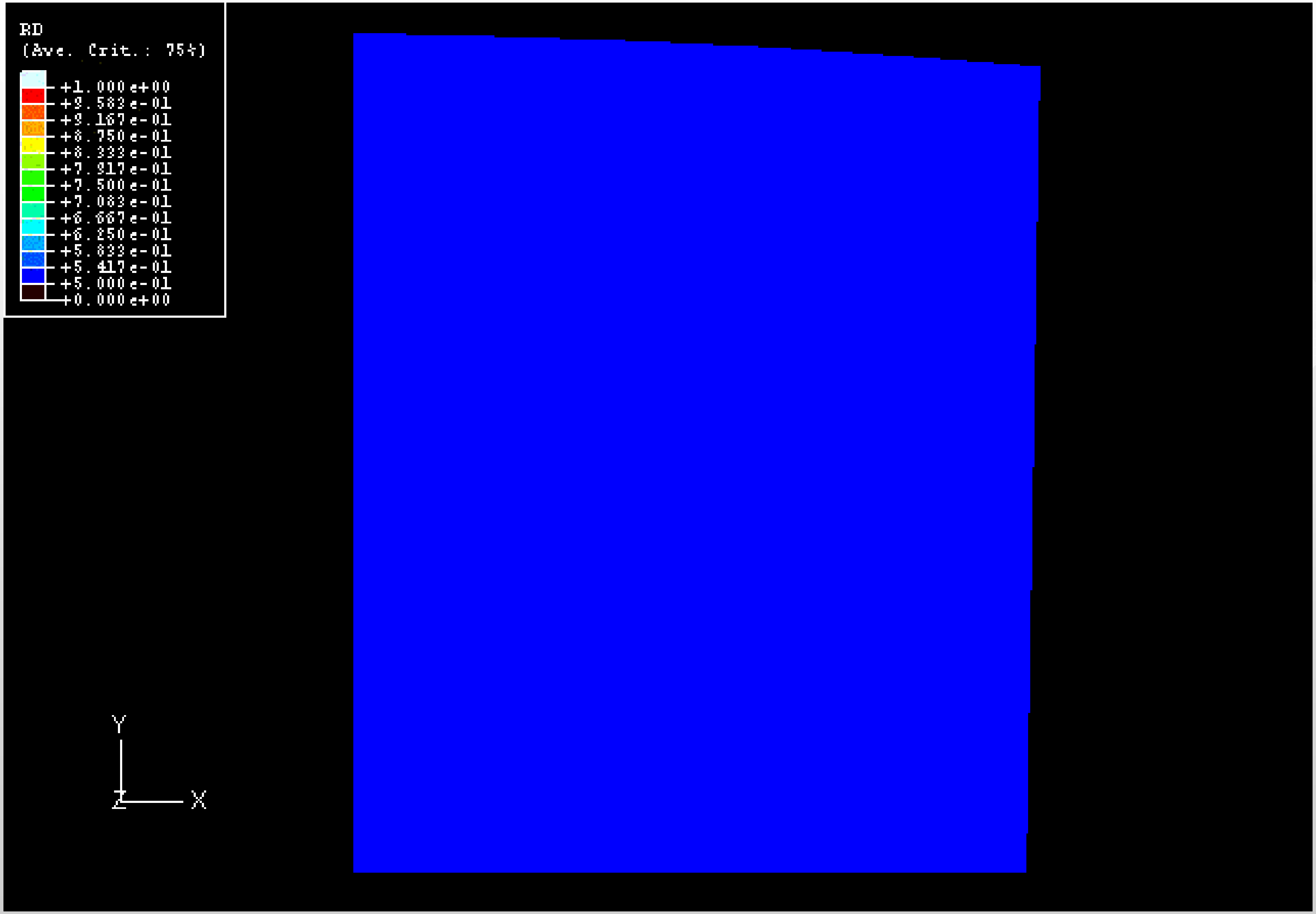

Conclusions

Conclusion (Theoretical Modeling)

1. **Modeling of pressing of porous materials in a rigid die shows that the Skorohod model for bulk modulus and shear modulus and power law creep material constitutive behavior of the material have the best agreement with the experimental results.**
2. **As a first approximation, PTM can be modeled as an elastic material. The elastic constitutive behavior of the PTM can be modeled as a function of composition of fused alumina and graphite in the PTM and the porosity of the PTM.**
3. **Densification and distortion of the porous combustion reacted material were successfully modeled. An optimal composition of 75%wt. fused alumina and 25%wt. graphite was chosen for the purpose of QIP applications in further studies.**

Conclusion (Experiments)

1. **A mole composition between *Ti*:*C* = 1.4:1.0 and *Ti*:*C* = 1.6:1.0 gives the best final product from the viewpoint of morphology and mechanical properties. For the purpose of obtaining a high hardness final product, the mole ratio of *Ti*:*C* = 1.4:1.0 is used in further investigations.**
2. **Based on the experiments and former study results, a consolidation load of 50 to 70 tons is found to be the proper load in order to obtain dense final products.**
3. **A time window less than 5 seconds between combustion and consolidation is proposed. A preload combustion system is designed for this purpose.**
4. **Small size C particles result in more intensive reaction and more cracks in final products.**
5. **A low melting temperature metallic binder helps decreasing cracks and improving mechanical properties of final products.**

Conclusion (FEM Simulation)

1. **A finite element model, where the porous combustion reacted material was modeled as a power law creep material and the PTM was modeled as a rigid-plastic granular material, was created. The simulation results show similar deformation and distortion of the combustion reacted material to experiment results.**
2. **Both the Mohr-Coulomb and Drucker-Prager/Cap models are used for modeling of constitutive behavior of PTM with acceptable agreement of experimental results.**
3. **An optimized initial shape for obtaining of a net-shape final product is obtained**

Published/Submitted Papers

- J. Ma, E.A. Olevsky, and M.A. Meyers, Modeling of Densification of Porous and Ductile Cermet Composites, Proc. 2001 NSF Design, Service & Manufacturing Grantees & Research Conference (EPP CD-ROM Proceedings), 8p., Tampa, Florida (2001).
- J. Ma, E.A. Olevsky and M.A. Meyers, Densification of Cermet Composites, PM2 TECH Papers A37 (2001).
- M.A. Meyers, E.A. Olevsky, J. Ma, and J.M. Jamet, Combustion Synthesis /Densification of an Al2O3-TiB2 Composite, Mater. Sci. Eng. A, Volume 311, Issues1-2, 31 July 2001, Pages 83-99.
- 2nd Place Award, 16th Annual CSU Student Research Competition Engineering Group (2002).
- E.A. Olevsky, J.C. LaSalvia, J. Ma, and M.A. Meyers, Densification of Porous Bodies in a Granular Pressure-Transmitting Medium: Part I, Shrinkage Anisotropy, Submitted to Acta Materialia (2004).
- E.A. Olevsky, J.C. LaSalvia, J. Ma, and M.A. Meyers, Densification of Porous Bodies in a Granular Pressure-Transmitting Medium: Part II, Shape Distortion, Submitted to Acta Materialia (2004).

Suggested Future Works

1. **Analysis of the thermodynamics of combustion synthesis: solution of a coupled heat transfer – densification problem.**
2. **Applications to nano-materials (recently reported by Z.A. Munir *et al.* grain size retention during SHS).**
3. **Solution of inverse problems of QIP to obtain the desired final complex net-shape products.**
4. **Fabrication of functionally graded composite combustion-synthesized cermets.**

Questions?